GUT MICROBES
2025, VOL. 17, NO. 1, 2474149
https://doi.org/10.1080/19490976.2025.2474149

Taylor & Francis
Taylor & Francis Group

RESEARCH PAPER

OPEN ACCESS Check for updates

Isolation of derivatives from the food-grade probiotic *Lactobacillus johnsonii* CNCM I-4884 with enhanced anti-*Giardia* activity

Anne-Sophie Boucard[a], Saulius Kulakauskas[a], Jana Alazzaz[b], Soraya Chaouch[b], Mohamed Mammeri[c], Aaron Millan-Oropeza[d], Carine Machado[d], Céline Henry[d], Christine Péchoux[e], Holger Richly[f], Michael Gassel[f], Philippe Langella[a], Bruno Polack[c], Isabelle Florent[b], and Luis G. Bermúdez-Humarán[a]

[a]Département Adaptation du Vivant, Université Paris-Saclay, INRAE, AgroParisTech, Micalis Institute, Jouy-en-Josas, France; [b]UMR 7245, Muséum National d'Histoire Naturelle, Centre National de la Recherche Scientifique, Sorbonne Universités, Paris, France; [c]Anses, INRAE, Ecole Nationale Vétérinaire d'Alfort, UMR BIPAR, Laboratoire de Santé Animale, Maisons-Alfort, France; [d]Plateforme d'Analyse Protéomique Paris Sud-Ouest (PAPPSO), INRAE, MICALIS Institute, Université Paris-Saclay, Jouy-en-Josas, France; [e]Université Paris-Saclay, INRAE, AgroParisTech, GABI, Jouy-en-Josas, France; [f]Boehringer Ingelheim Vetmedica GmbH, Kathrinenhof Research Center, Rohrdorf, Germany

ABSTRACT

Giardiasis, a widespread intestinal parasitosis affecting humans and animals, is a growing concern due to the emergence of drug-resistant strains of *G. intestinalis*. Probiotics offer a promising alternative for preventing and treating giardiasis. Recent studies have shown that the probiotic *Lactobacillus johnsonii* CNCM I-4884 inhibits *G. intestinalis* growth both *in vitro* and *in vivo*. This protective effect is largely mediated by bile salt hydrolase (BSH) enzymes, which convert conjugated bile acids (BAs) into free forms that are toxic to the parasite. The objective of this study was to use adaptive evolution to develop stress-resistant derivatives of *L. johnsonii* CNCM I-4884, with the aim of improving its anti-*Giardia* activity. Twelve derivatives with enhanced resistance to BAs and reduced autolysis were generated. Among them, derivative M11 exhibited the highest *in vitro* anti-*Giardia* effect with enhanced BSH activity. Genomic and proteomic analyses of M11 revealed two SNPs and the upregulation of the global stress response by SigB, which likely contributed to its increased BAs resistance and BSH overproduction. Finally, the anti-*Giardia* efficacy of M11 was validated in a murine model of giardiasis. In conclusion, our results demonstrate that adaptive evolution is an effective strategy to generate robust food-grade bacteria with improved health benefits.

ARTICLE HISTORY
Received 15 August 2024
Revised 3 January 2025
Accepted 25 February 2025

KEYWORDS
Lactobacillus johnsonii; probiotic; *Giardia intestinalis*; giardiasis; Bile salt hydrolases

Introduction

Giardia intestinalis is the protozoan responsible for giardiasis, a widespread intestinal infection affecting humans and animals.[1] Acute giardiasis is characterized by intestinal malabsorption, diarrhea, abdominal pain, nausea, vomiting and weight loss. In humans, giardiasis can lead to post-infectious complications, such as irritable bowel syndrome (IBS), chronic fatigue and growth retardation.[2–4] Treatment of *G. intestinalis* infection usually consists of nitroimidazoles or benzimidazoles. However, failure rates range from 5% to 50%, and resistance to these drugs has increased in the last 15 years.[5–7] Alternative strategies to control *G. intestinalis* infections include the repurposing of approved drugs and structural modifications of nitroimidazoles and benzimidazoles,[5,8] the use of polyphenols derived from medicinal plants, including ginger and curcumin[9,10] and animal-derived compounds such as lactoferrin and propolis.[11,12]

Given the close association between gut microbiota composition and susceptibility to *G. intestinalis* infection,[13,14] probiotics (*live microorganisms that, when administered in adequate amounts, confer a health benefit on the host*[15]) represent a promising alternative strategy for the prevention and treatment of giardiasis. Indeed, the administration of probiotics has showed protective effect against a number of pathological conditions, including IBS,[16] inflammatory bowel disease (IBD),[17] metabolic syndrome[18] and SARS-CoV2 infection,[19] among others. However, there is a paucity of studies reporting the efficacy of probiotics in controlling *G. intestinalis* infection. To date,

CONTACT Luis G. Bermúdez-Humarán luis.bermudez@inrae.fr Université Paris-Saclay, INRAE, AgroParisTech, Micalis Institute, Jouy-en-Josas 78350, France

the efficacy of probiotics alone has only been demonstrated *in vitro*[20] and *in vivo* in preclinical rodent models.[21–23] Two clinical trials demonstrated the protective effect of probiotic *Enterococcus faecium* SF68 and *Saccharomyces boulardii*, when administered in combination with metronidazole therapy in dogs[24] and humans,[25] respectively. The protective effect of probiotics in *G. intestinalis* infection may involve different mechanisms, including stimulation of the host immune response to enhance the production of nitric oxide, IgA and IgG,[26–28] secretion of bacteriocin[29] or stimulation of host mucus production.[21,30]

The probiotic strain *Lactobacillus johnsonii* CNCM I-4884 (formerly classified as *Lactobacillus gasseri*) has been shown to significantly inhibit *G. intestinalis* proliferation in a murine model of giardiasis.[31] In addition, we recently demonstrated that the protective effect of *L. johnsonii* CNCM I-4884 is mediated by its production of bile salt hydrolase (BSH) enzymes, which convert conjugated bile acids (BAs), major bile components essential for *G. intestinalis* growth, into free BAs, which are toxic to the parasite (Boucard et al., manuscript in preparation).

The main objective of this study was to use adaptive laboratory evolution to develop derivatives of *L. johnsonii* CNCM I-4884, with the aim of enhancing anti-*Giardia* properties of the strain. A collection of 12 mutants exhibiting increased resistance to BAs and reduced autolysis was generated and initially screened for their anti-*Giardia* activity on *G. intestinalis* trophozoite cultures. Three derivatives, M3, M5 and M11, were selected for further characterization of their growth, adhesion to intestinal cell lines, biofilm formation, morphology, BSH activity, and whole genome sequence. It is important to highlight that these derivatives were generated without molecular biology techniques and may thus be considered as food-grade microorganisms. The most promising candidate, M11, was also characterized at the proteomic level, and its protective effect was investigated *in vivo* in a murine model of giardiasis.

Results

Screening of stress-resistant derivatives of L. johnsonii *CNCM I-4884*

The strategy to generate stress-resistant derivatives involved three selective pressures, as shown in Figure 1a. Lactobacilli are naturally sensitive to BAs. It has been described that the production of BSH can confer enhanced resistance to BAs. Therefore, the main objective of this screening strategy was to generate derivatives with improved resistance to both free and conjugated BAs, potentially enhancing BSH production and improving persistence in the host. To do so, isolated clones of *L. johnsonii* CNCM I-4884 wild-type were grown on three successive gradients of MRS medium with increasing concentrations of cholic acid (CA) and deoxycholic acid (DCA). This lead to isolation of four clones, designated M1 to M4, that displayed increased resistance compared to wild-type. In the second screen, *L. johnsonii* CNCM I-4884 wild-type was grown on THY semi-liquid medium to isolate clones with modified surface properties. Under these conditions, single cell bacteria sediment and form prolonged colonies. In contrast, bacteria forming chains and aggregates are immobilized and do not sediment, and thus are easily distinguishable. Since bacterial chains often correspond to cell separation defects due to the robustness of their cell wall, such clones are expected to have reduced autolysis.[32] Clones with delayed sedimentation were tested for resistance to autolysis in phosphate buffer containing 0.05% Triton X-100. Three derivatives (M5 to M7) showed significantly reduced autolysis compared to wild-type ($p < 0.001$; $p = 0.002$; $p = 0.040$, respectively). Finally, M1 to M7 candidates from the initial screens were grown on gradients of taurodeoxycholic acid (TDCA) and glycodeoxycholic acid (GDCA) to select derivatives resistant to conjugated BAs. This step yielded five additional resistant clones (M8 to M12) with increased tolerance to BAs compared to wild-type. Clones M8 to M10 were from autolysis-resistant M7, whereas M11 and M12 were from M4 derivative resistant to unconjugated BAs.

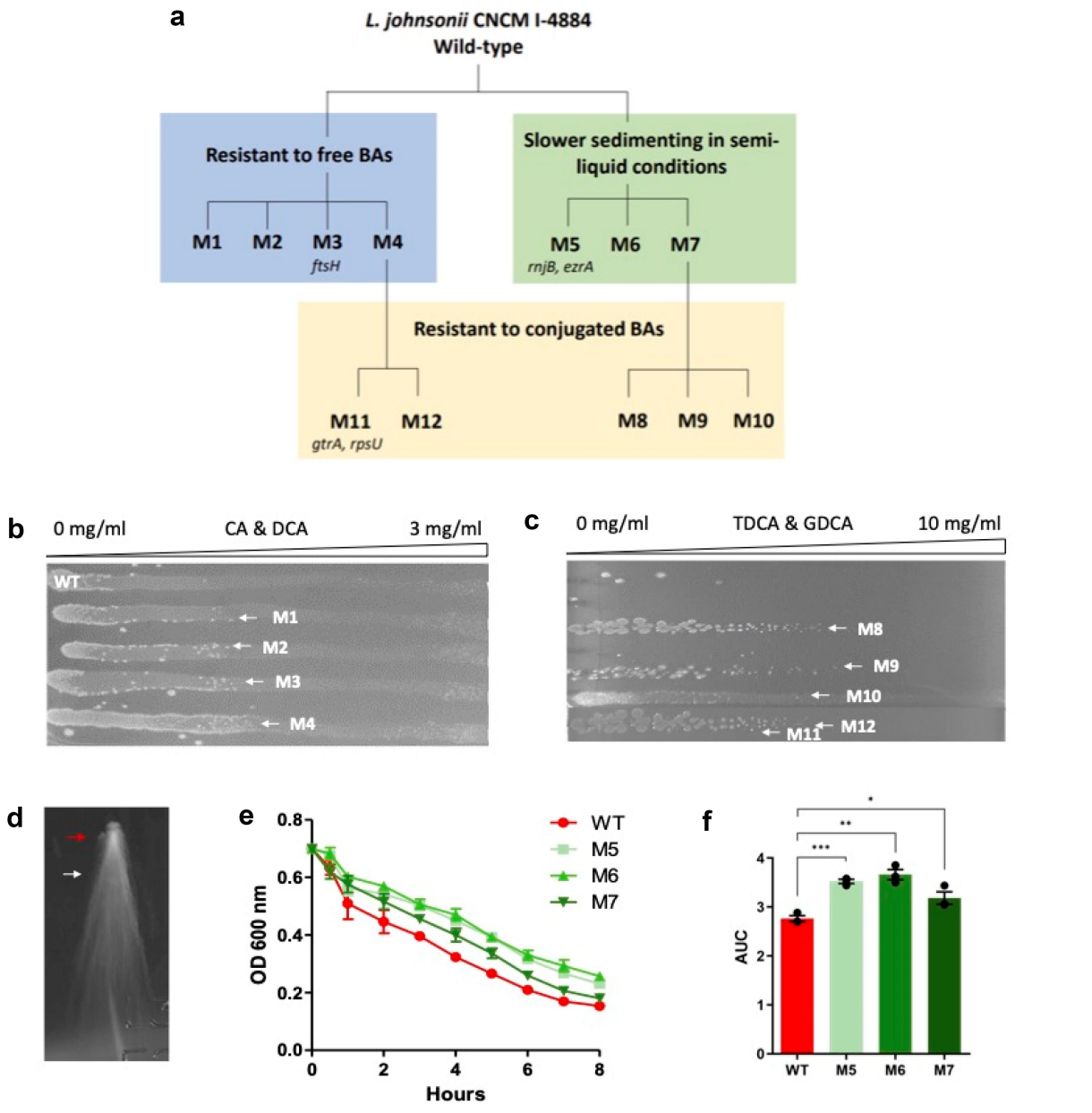

Figure 1. Screening and characterization of derivatives of *L. johnsonii* CNCM I-4884. (a) Schematic representation of the derivatives selection process. Refer to section "*whole genome sequencing*" for details on mutation identification. (b) Clones resistant to free BAs were selected using CA and DCA gradients. (c) Clones resistant to conjugated BAs were selected on TDCA and GDCA gradients. (d) Clones with altered sedimentation profiles were selected on THY + 0.03% agar; white arrow shows elongated wild-type colonies, red arrow points to slower sedimenting mutants with round colonies. (e) Autolysis was assessed by OD 600 nm in K_2HPO_4/KH_2PO_4 buffer + 0.05% triton X-100; data are shown as mean ± SEM ($n = 3$). (f) Area under curve of OD 600 nm. Asterisks indicate statistical significance compared to wild-type, as determined with unpaired *t*-test (***$p < 0.001$; **$p < 0.01$; *$p < 0.05$).

*In vitro anti-*Giardia *activity*

To assess the anti-*Giardia* activity of *L. johnsonii* CNCM I-4884 wild-type and derivatives, *G. intestinalis* trophozoites were incubated with different concentrations of bacterial culture supernatants. After 22 h, viable trophozoites were counted and compared to untreated parasite cultures. Undiluted culture supernatants from all *L. johnsonii* strains reduced trophozoite viability (Figure 2a). Moreover, the M3 and M11 undiluted supernatants showed significantly higher levels of parasite growth inhibition than undiluted wild-type supernatant, with 0.1% and 0.0% viable trophozoites compared to 6.5% for wild-type ($p = 0.032$ and $p = 0.028$, respectively). In

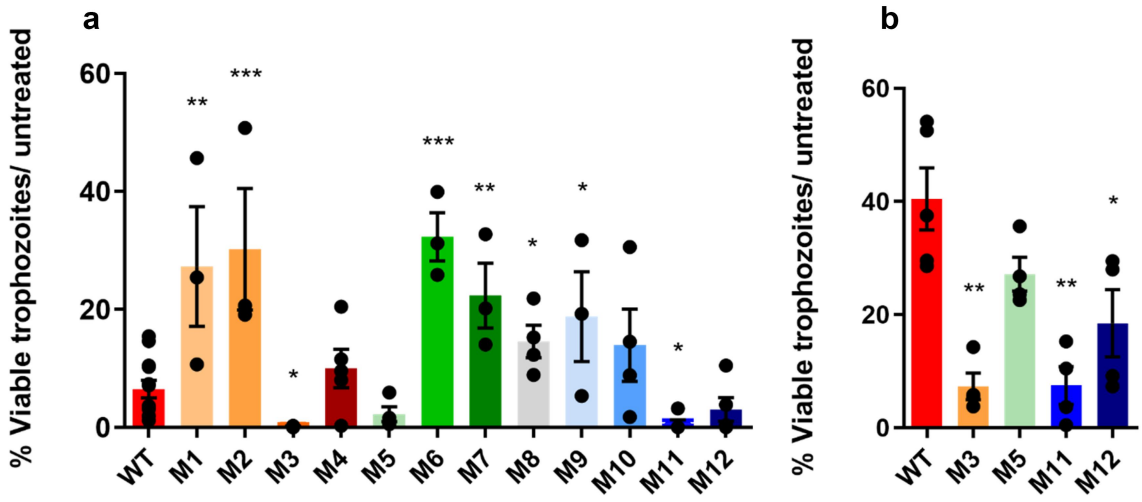

Figure 2. Growth inhibition of *G. intestinalis* trophozoites by culture supernatants of *L. johnsonii* CNCM I-4884 wild-type and derivatives relative to untreated parasite cultures, tested as undiluted (a) and 1/2 diluted (b) bacterial supernatants. Values are mean ± SEM ($n = 4$). Asterisks indicate statistical significance compared to wild-type, as determined with unpaired *t*-test (***$p < 0.001$; **$p < 0.01$; *$p < 0.05$).

the presence of ½ diluted supernatant, M3 and M11 still showed a significant enhanced inhibitory activity, with 7.3% ($p = 0.002$) and 7.5% ($p = 0.002$) live trophozoites, respectively, compared to 40.5% for wild-type. M5 also showed increased inhibitory activity with 27.1% live trophozoites, but the difference with wild-type did not reach statistical significance (Figure 2b).

Bacterial growth rates

The M3, M5, and M11 derivatives, i.e., one from each screen, were selected for further phenotypic characterization relative to wild-type. First, their growth rates were assessed over 30 h at 37°C, in absence or presence of a mix of conjugated BAs (TDCA and GDCA). In MRS medium, M3 and M11 showed significantly reduced or retarded growth rate compared to wild-type ($p = 0.022$ and $p = 0.002$, respectively) (Figure 3a,b). However, in the presence of conjugated BAs, the growth rates of all three derivatives were significantly improved compared to wild-type ($p = 0.003$, $p = 0.013$ and $p = 0.015$, respectively) (Figure 3c,d).

Adhesion to intestinal cell lines

Certain probiotic strains have the ability to adhere to the intestinal mucosa or the upper mucus layer, which may enhance their capacity to exert beneficial effects on the host. The adhesive properties of *L. johnsonii* CNCM I-4884 wild-type and derivatives were tested *in vitro* on four intestinal cell lines, using *Lacticaseibacillus rhamnosus* strain GG (LGG) as a positive control (Figure 4). The wild-type strain showed adhesion comparable to LGG on Caco-2, HT-29 MTX and T84 cell lines, and significantly higher adhesion on HT-29 cell line ($p = 0.003$). The derivatives showed similar or higher adhesion capacity than LGG for the four cell lines tested. Notably, M11 showed significantly improved adhesion to Caco-2 ($p < 0.001$), HT-29 ($p < 0.001$) HT-29 MTX ($p = 0.030$) and T84 ($p = 0.019$) cell lines compared to LGG.

Biofilm formation

Biofilms are bacterial communities of surface-attached bacteria embedded in an extracellular matrix. Through the gastrointestinal tract (GIT), biofilms grow naturally on both the epithelial surface and in the lumen as colonies attached to mucin and food particles.[33] The ability of *L. johnsonii* CNCM I-4884 wild-type and derivatives to form biofilms *in vitro* was investigated using confocal microscopy. As shown in Figure 5, the wild-type strain formed an homogeneous biofilm that adhered effectively to the well surface. In contrast, M3, M5, and M11 derivatives formed thicker and

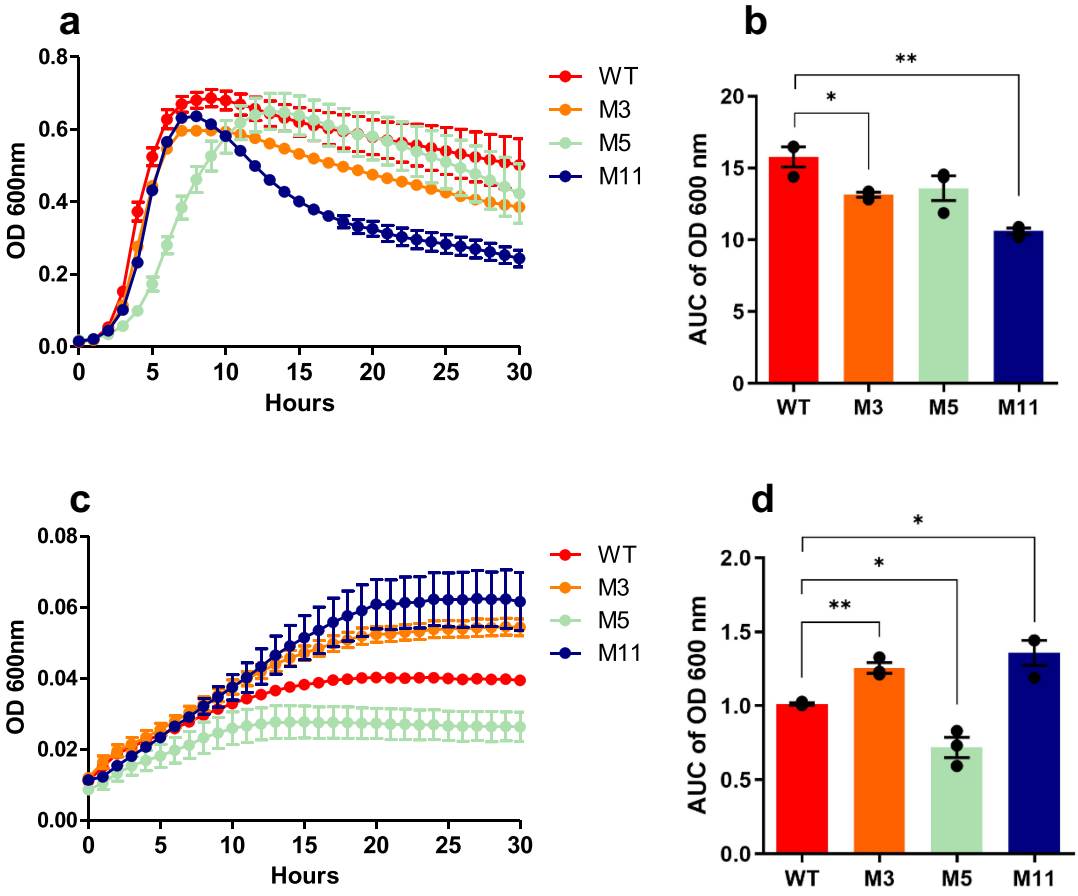

Figure 3. Growth rates of *L. johnsonii* CNCM I-4884 wild-type and derivatives in MRS medium (a) and area under curve (b) or MRS supplemented with a mix of conjugated BAs (1 mg/ml TDCA and GDCA) (c) and area under curve (d). Data are represented as mean ± SEM ($n = 3$). Asterisks indicate statistical significance compared to wild-type, as determined with unpaired *t*-test (**$p < 0.01$; *$p < 0.05$).

denser mature biofilms, with a corresponding increase of biovolume ($p < 0001$; $p < 0001$ and $p < 0001$, respectively). Notably, M11 showed the highest biofilm formation, probably linked to its higher adhesive capacity, as shown in Figure 4. Consistent with previous findings, this increased adhesion and biofilm formation may provide M11 with a greater ability to persist *in vivo* by transiently colonizing the mucosal layer and/or intestinal epithelium, thus enhancing its probiotic effects.[34–36]

TEM observations

Given that some derivatives displayed altered sedimentation profile in semi-liquid medium and reduced autolysis, potentially indicating modified surface properties, the cell wall (CW) structure of *L. johnsonii* CNCM I-4884 wild-type and derivatives was investigated by TEM (Figure 6). M3 and M11 exhibited a morphology similar to the wild-type strain, with an average cell lenght of 9 µm. In contrast, variant M5 presented elongated cells (14 µm), with a thicker, irregular CW (45 nm) and numerous intracellular inclusions. Consistent with its altered sedimentation profile and decreased autolysis, M5 also presented an irregular CW which is significantly thicker than wild-type ($p < 0.001$).

Whole genome sequencing

The complete genomes of M3, M5, and M11 derivatives were sequenced, assembled, and compared to the genome of *L. johnsonii* CNCM I-4884 wild-type[37] to identify genetic differences. Overall, 1, 2, and 2 mutations were identified in the coding regions of M3, M5, and M11 genomes, respectively. The M3 genome revealed a missense mutation in *ftsH* gene, which encodes a membrane-anchored zinc metalloprotease with dual chaperone-

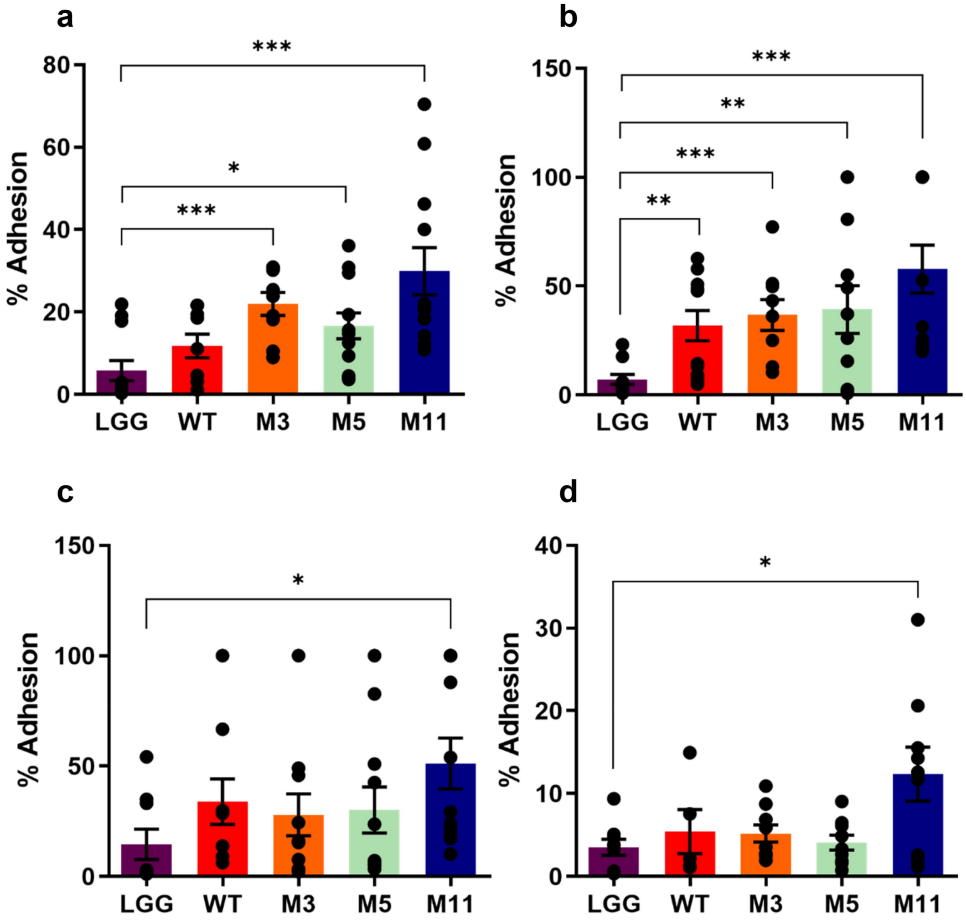

Figure 4. Adhesion of *L. johnsonii* CNCM I-4884 wild-type and derivatives to Caco-2 (a), HT-29 (b), HT-29 MTX (c) and T84 cell lines (d). Data are represented as mean ± SEM ($n = 12$). Asterisks indicate statistical significance compared to LGG, as determined with unpaired *t*-test (*$^{***}p < 0.001$; $^{**}p < 0.01$; $^{*}p < 0.05$).

protease activities. FtsH plays an important role in bacterial stress response mechanism, enabling rapid proteome adaptation to withstand harsh conditions and sudden environmental changes.[38–40] In *Lactiplantibacillus plantarum*, FtsH expression is significantly upregulated in response to various stress conditions, including heat, oxidative and bile stress.[41] FtsH has been proposed to impact the physicochemical properties of the cell surface, either directly or indirectly.[42] In *Escherichia coli*, the challenges associated with obtaining a viable FtsH-null mutant suggest that FtsH is essential for survival in this species.[38] Conversely, in Gram-positive bacteria, FtsH is not considered essential. Nonetheless, loss of FtsH function in both *L. plantarum* and *L. rhamnosus* leads to reduce growth rates under normal conditions, with the growth impairment becoming more pronounced under stress conditions.[43,44] In contrast, a genetically modified *L. plantarum* overexpressing FtsH showed improved growth in the presence of bile.[42] In M3, the mutation resulted in a replacement of an alanine (Ala) residue by a valine (Val) at position 53 within the periplasmic region of FtsH, a critical site for proper regulation of substrate selection. As shown in Figure 3, M3 growth is delayed under standard conditions but is improved in the presence of BAs. Furthermore, key residues within ATPase and protease domains of FtsH are conserved, indicating that the mutation should not compromise protein functionality. In M3, the FtsH mutation in the substrate recognition domain may enhance its substrate binding or proteolytic activity, resulting in improved resistance to BAs. In addition, indirect observations suggest a putative function of FtsH in modulating the CW architecture of *Lactococcus lactis*,[45] which may explain the thicker CW observed in M3.

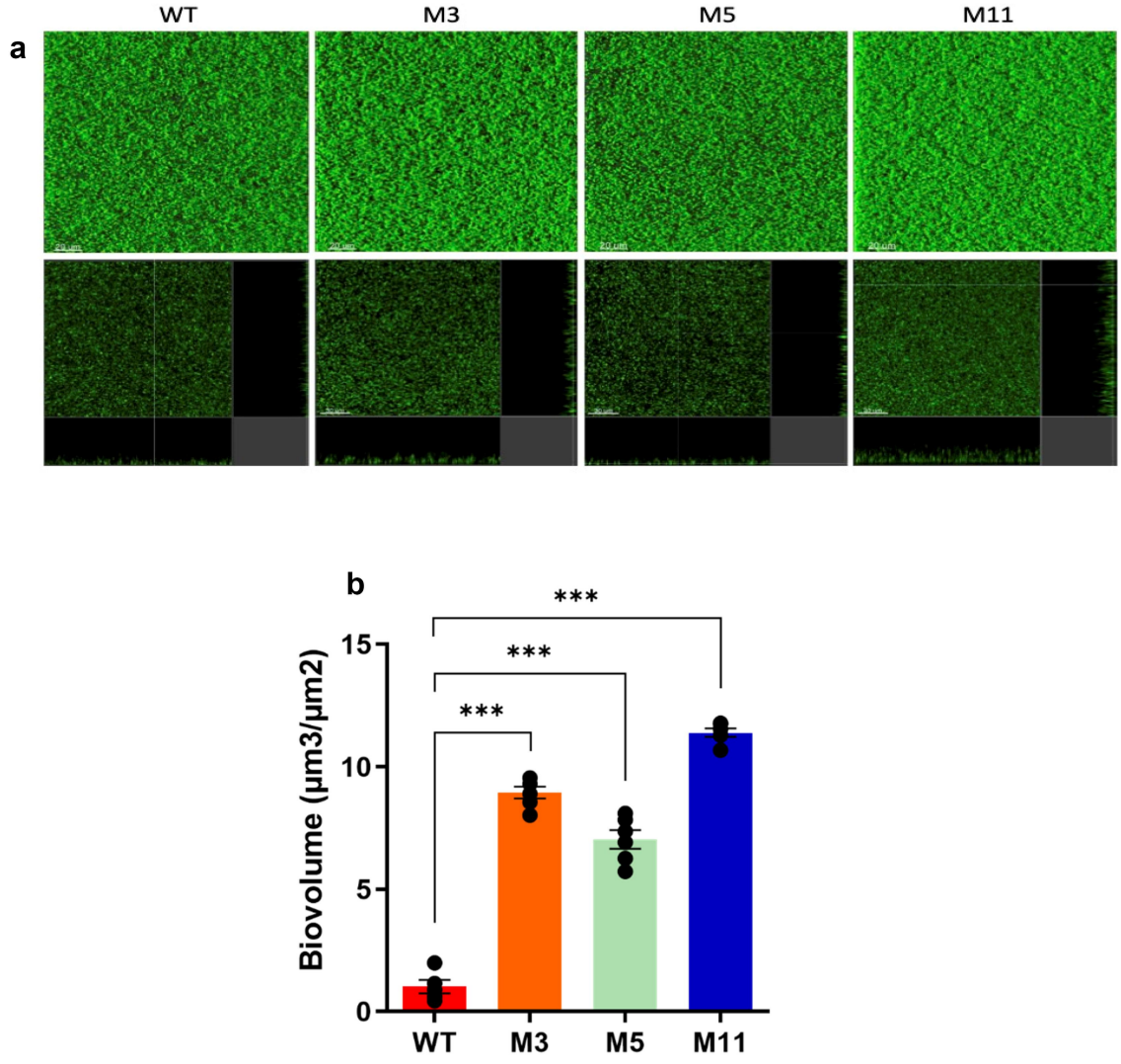

Figure 5. Biofilm formation by *L. johnsonii* CNCM I-4884 wild-type and derivatives. (a) 3D projections and section views of biofilm structure obtained from confocal z-stacks using IMARIS software; white scale bars represent 20 µm (b) quantification of biofilm biovolume. Data are presented as mean ± SEM ($n = 6$). Asterisks indicate statistical significance compared to wild-type, as determined with unpaired *t*-test (***$p < 0.001$).

The M5 genome presents a mutation that introduces a premature stop codon in the *rnjB* gene encoding J2 ribonuclease. Ribonucleases J1 and J2 play roles in degradation of messenger RNA and maturation of non-coding RNA.[46,47] The entire *rnjA* gene, encoding ribonuclease J1, remains intact in the M5 genome. These two enzymes are paralogs with conserved function; however, gene knockout in *Bacillus subtillis* has shown that RNase J1 (*rnjA*) is essential, whereas RNase J2 (*rnjB*) is not.[48] This suggests that the loss of RnjB functionality in M5 may be compensated for by the presence of RnjA, and most probably would not affect M5 phenotype. A second mutation in M5 was identified in the *ezrA* gene, altering a glutamate (Glu) residue to an aspartate (Asp) at the C-terminal end of the protein. EzrA is a membrane-associated protein coordinating cell division and cell wall synthesis. During the cell cycle, the cell division protein FtsZ forms a ring structure that determines the site of nascent division. EzrA acts as a negative regulator of FtsZ, modulating both the frequency and precise position of FtsZ ring formation.[49] This mutation could be responsible for the elongated cell shape and multiple inclusions at polar and medial sites observed in TEM images (Figure 6), a phenotype similar to that described in knockout mutants of *Bacillus subtilis* and *L. plantarum*.[49–51]

The M11 genome contains a missense mutation in the *gtrA* gene, resulting in a change of serine

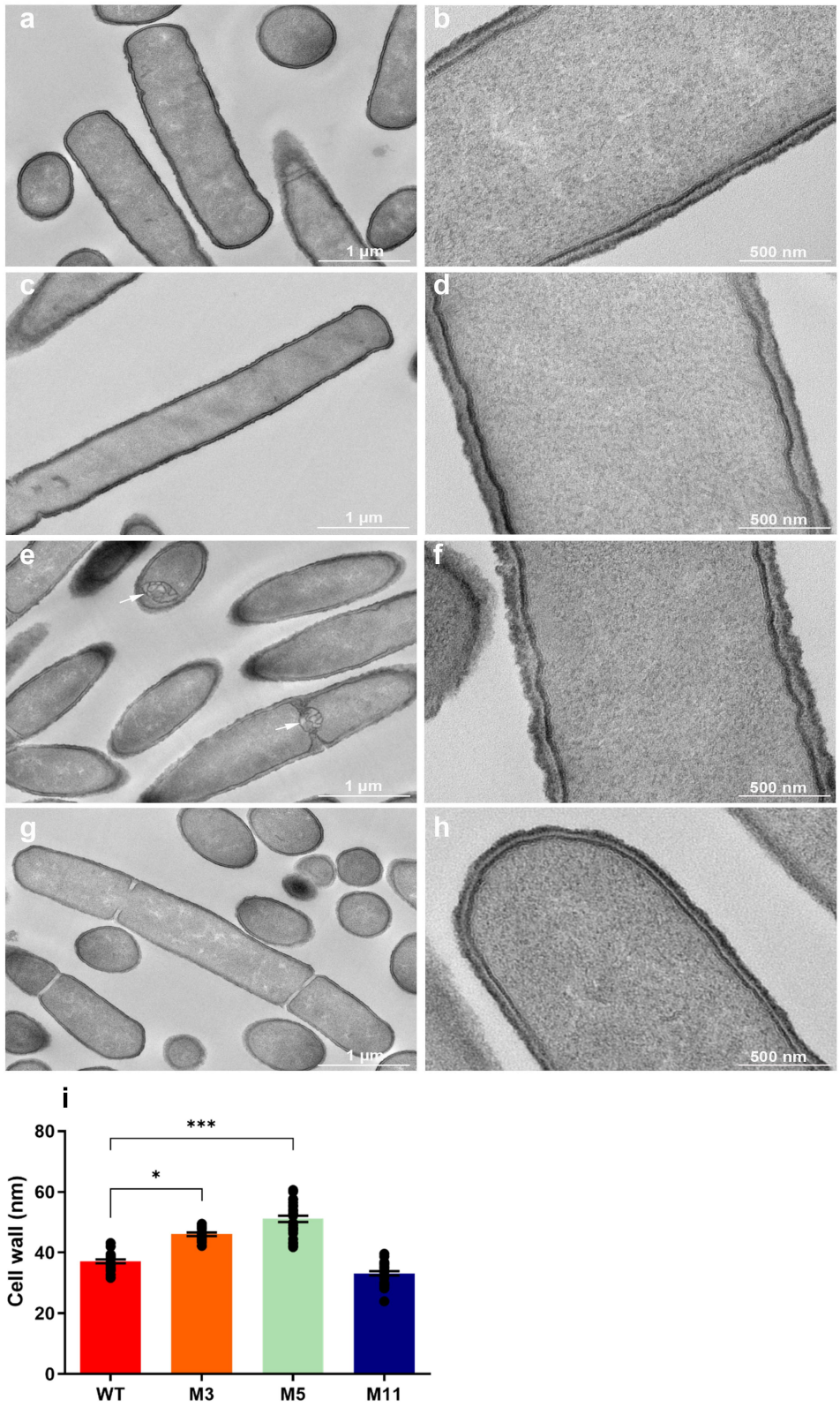

Figure 6. TEM observations of *L. johnsonii* CNCM I-4884 wild-type (a, b), and M3 (c, d), M5 (e, f) and M11 (g, h) derivatives, fixed in exponential growth phase. Inclusions (in M5) are indicated with an arrow. (i) Cell wall thickness. Data are represented as mean ± SEM (n = 15 to 30). Asterisks indicate statistical significance compared to wild-type as determined with unpaired t-test (***$p < 0.001$; *$p < 0.05$).

(Ser) to a tyrosine (Tyr) at position 114. The *gtrA* gene encodes a putative flippase of the GtrA superfamily, involved in the production of branched glucan homopolysaccharide.[52] Exopolysaccharides (EPS), which protect bacterial surfaces and facilitate host interactions, create a more hydrophilic and less negatively charged surface, reducing cell self-aggregation. Compared to wild-type, M11 shows increased self-aggregation in liquid culture (data not shown), suggesting a loss of function in EPS biosynthesis.[52,53] Studies on EPS production have shown contradictory effects on stress resistance. For example, in *L. johnsonii* FI9785, reduced EPS production led to lower survival under stress conditions, whereas in *Bifidobacterium longum*, it improved acid tolerance.[53,54] Furthermore, decreased EPS production in *L. johnsonii* FI9785 and *L. johnsonii* La1 strains increased their adhesion to chicken gut explants[53] and improved their persistence in the murine GIT.[55] This suggests that M11, with altered EPS production, might also show better persistence in the GIT than the wild-type counterpart. Finally, the M11 genome also contains a missense mutation in *rpsU* gene, resulting in a change from a lysine (Lys) to an asparagine (Asn) at position 44. The *rpsU* gene encodes the 30S ribosomal protein S21p. Consistent with M11 stress-resistant phenotype, variants of *Listeria monocytogenes* affected in *rpsU* also presented an enhanced resistance to various stresses, including acid, cold and heat stress.[56] As with M11, *L. monocytogenes* variants showed slower growth rate and increased adhesion to Caco-2 cells compared to the wild-type.[57]

Bile salt hydrolase activity

To determine whether the higher anti-*Giardia* activity observed in the stress-resistant derivatives was related to higher BSH production, the strains were exposed to a panel of tauro- and glycoconjugated BAs. BSH activity was assessed by measuring the levels of conjugated and free BAs by HPLC MS/MS. All four strains, including the wild-type and the three derivatives, demonstrated the ability to hydrolyze a wide range of conjugated BAs commonly found in humans and other mammals (Figure 7). In particular, M11 showed significantly higher hydrolytic activity than wild-type for all tauroconjugated BAs tested, as well as for several glycoconjugated BAs, including GCDCA, GDCA, and GCA. The higher BSH activity of M11 is consistent with its increased BAs resistance and higher anti-*Giardia* activity observed *in vitro* (Figures 1,2). Altogether, these results led to the selection of M11 candidate for further characterization.

Proteomic analysis

In order to elucidate the impact of M11 mutations on its metabolism, wild-type and M11 proteomes were analyzed by LC-MS/MS in exponential and stationary culture growth phases. Based on the identified peptides, a total of 746 proteins were identified in wild-type and M11, representing 41.35% of the theoretical proteome. Data treatment resulted in 660 valid proteins quantified by XIC (extracted ion chromatograms). Principal component analysis (PCA) based on the 660 proteins revealed that samples were grouped by strain and growth phase (Figure 8a). For each growth phase, wild-type and M11 proteomes were compared to identify proteins with significantly different abundances. In exponential growth phase, 198 proteins were differentially expressed in M11 compared to wild-type, representing 26.5% of total proteins detected, among which 51 proteins were up-regulated and 147 were down-regulated with a log2 fold change ≥ 2 ($p \leq 0.05$). In stationary growth phase, 104 proteins were differentially abundant in M11 compared to wild-type, representing 13.9% of the proteins detected, among which 52 proteins were more abundant in M11 and 52 proteins were less abundant in M11 compared to wild-type. Proteins with statistically different abundance in the two strains are represented in a heatmap using hierarchical clustering with Euclidean distances (Figure 8b). The biological replicates grouped together, and the samples were clearly resolved in two main clusters corresponding to the two strains.

The Cluster of Orthologous Groups (COG) database was used to elucidate the function of differentially abundant proteins (Figure 8c,d). During exponential growth phase, the major molecular functions upregulated in M11 were isomerase, kinase, hydrolase and oxidoreductase activities involved in carbohydrates metabolism, nucleic acid

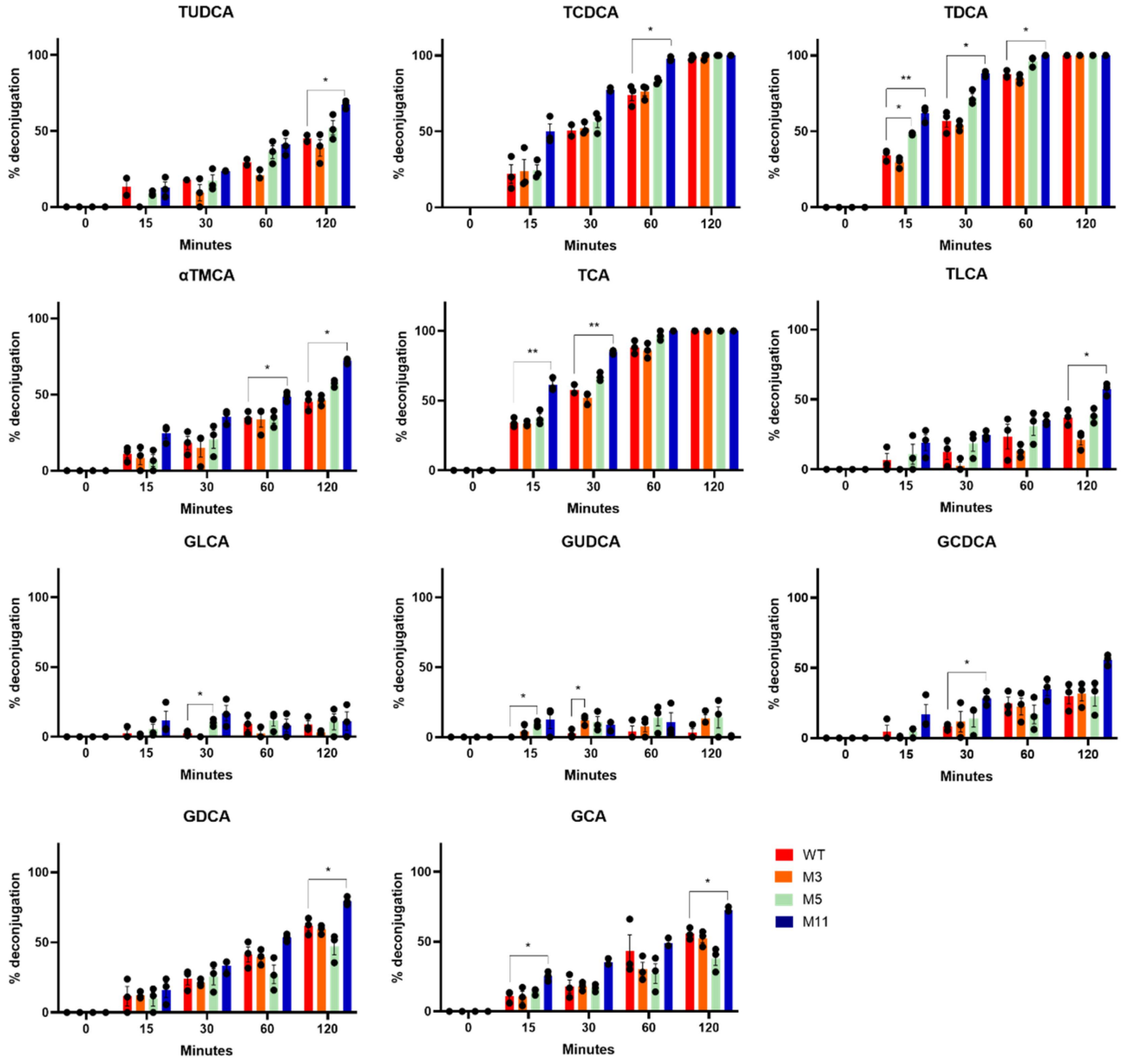

Figure 7. Bile acids (BAs) deconjugation activity of supernatant samples issued from cultures of *L. johnsonii* CNCM I-4884 wild-type and derivatives, after various incubation times. Data are represented as mean ± SEM ($n = 3$). Asterisks indicate statistical significance compared to wild-type, as determined with unpaired *t*-test (**$p < 0.01$; *$p < 0.05$). TUDCA : tauroursodeoxycholic acid; TCDCA : taurochenodeoxycholic acid; TDCA : taurodeoxycholic acid; αTMCA : tauromuricholic acid; TCA : taurocholic acid; TLCA : taurolithocholic acid; GLCA : glycolithocholic acid; GUDCA : glycoursodeoxycholic acid; GCDCA : glycochenodeoxycholic acid; GDCA : glycodeoxycholic acid; GCA : glycocholic acid.

metabolism, proteolysis and DNA repair. In contrast, downregulated molecular functions in M11 included mainly structural components of ribosome, rRNA and DNA binding, involved in transcription and translation. The same trend was observed in stationary growth phase samples.

The individual abundance of proteins belonging to the main cellular processes significantly different in M11 compared to wild-type are presented in Figure 9. Interestingly, BSH450 and BSH1011 enzymes were among the most overexpressed proteins in M11 compared to wild-type, with 3.11 and 3.94 log2 fold change, respectively, in exponential growth phase and with 2.63 and 3.18 log2 fold change, respectively, in stationary growth phase, which is consistent with the enhanced BSH activity of M11 observed in Figure 7. In addition, formyl-CoA transferase and

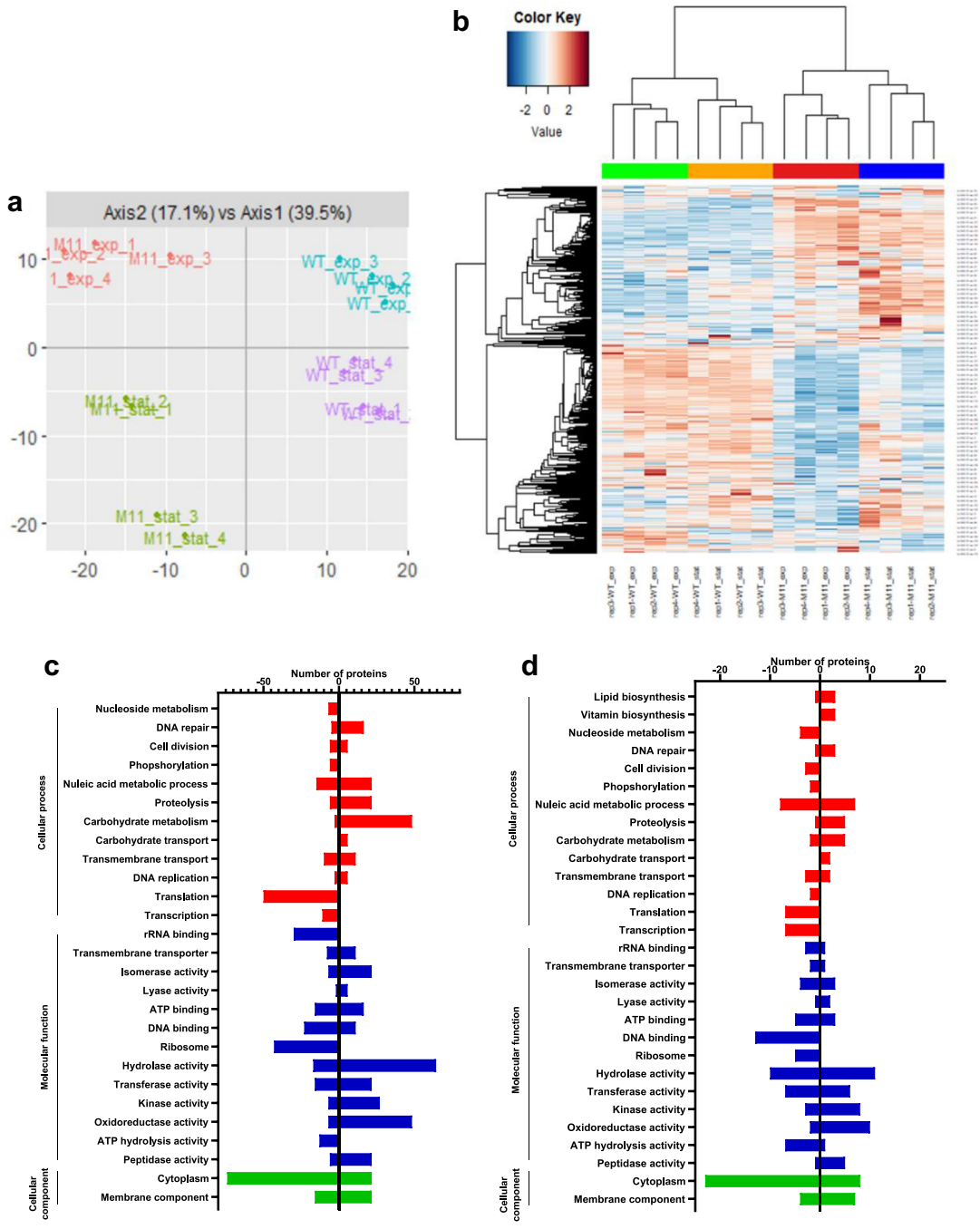

Figure 8. Proteomic analysis of *L. johnsonii* CNCM I-4884 wild-type and M11 derivative. (a) Principal component analysis. (b) Global heatmap representation of protein abundances significantly different in wild-type and M11 (n=4, ANOVA, adjusted p<0.05). Each row represents a differentially expressed protein, while each column represents a sample. (c) Functional classification based on GO enrichment analysis of differentially expressed proteins in exponential or (d) stationary growth phase.

oxalyl-CoA carboxylase, which are involved in oxalate metabolism, were among the most over-expressed proteins with 6.15 and 4.93 log2 fold change in exponential growth phase and overexpressed by 3.36 and 3.72 log2 fold change in stationary growth phase respectively.

In exponential growth phase, M11 samples showed a higher abundance of proteins involved in glycolysis, pentose phosphate pathway, pyruvate, nucleotide and nucleoside metabolisms. M11 also showed an increased abundance of proteins involved in cofactor biosynthesis, such as thiamine,

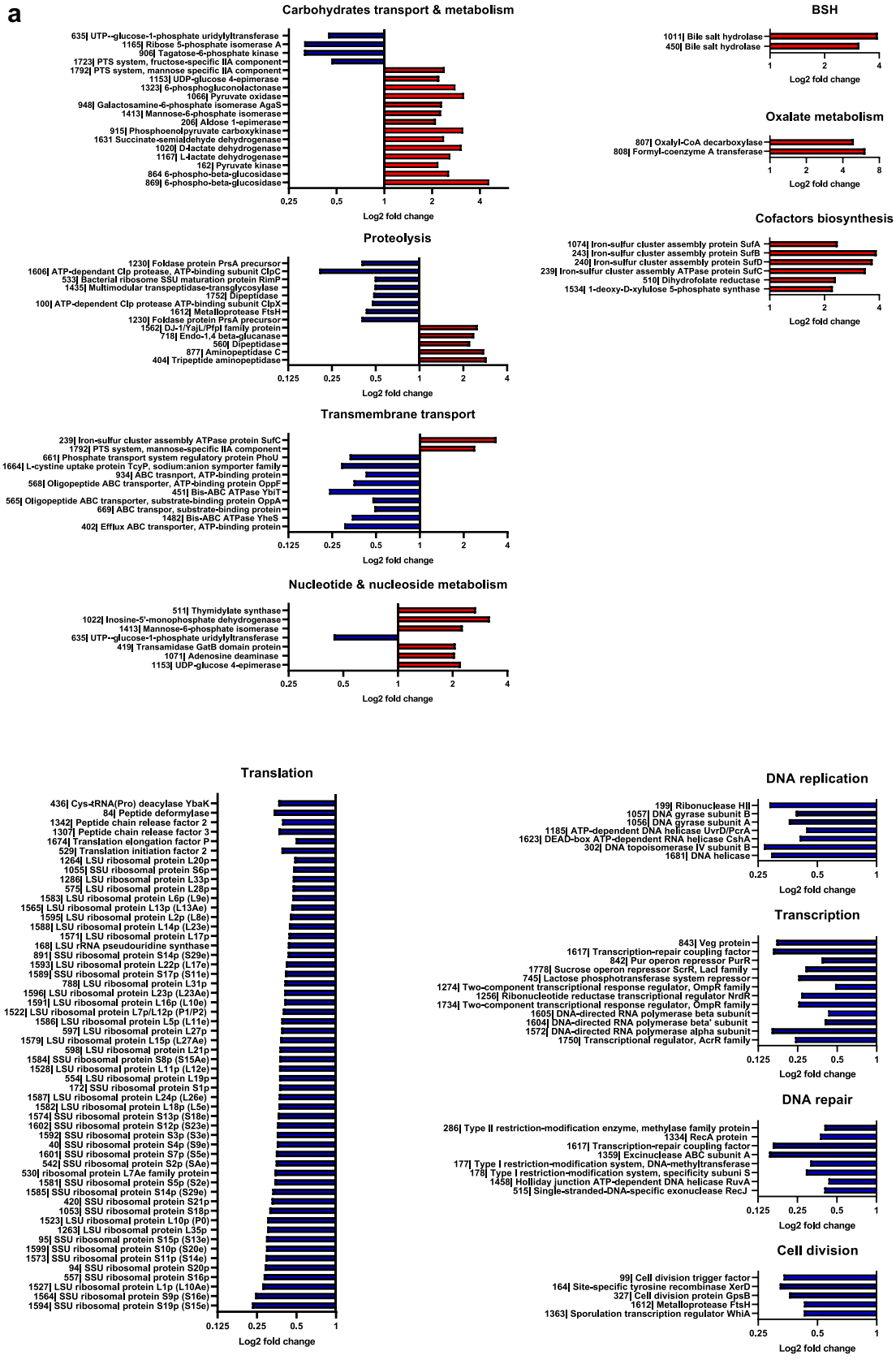

Figure 9. Fold-change of proteins with significant abundance change (ANOVA, adjusted $p<0.05$) between *L. johnsonii* CNCM I-4884 wild-type and M11 derivative, belonging to the main functional categories in (a) exponential and (b) stationary growth phase.

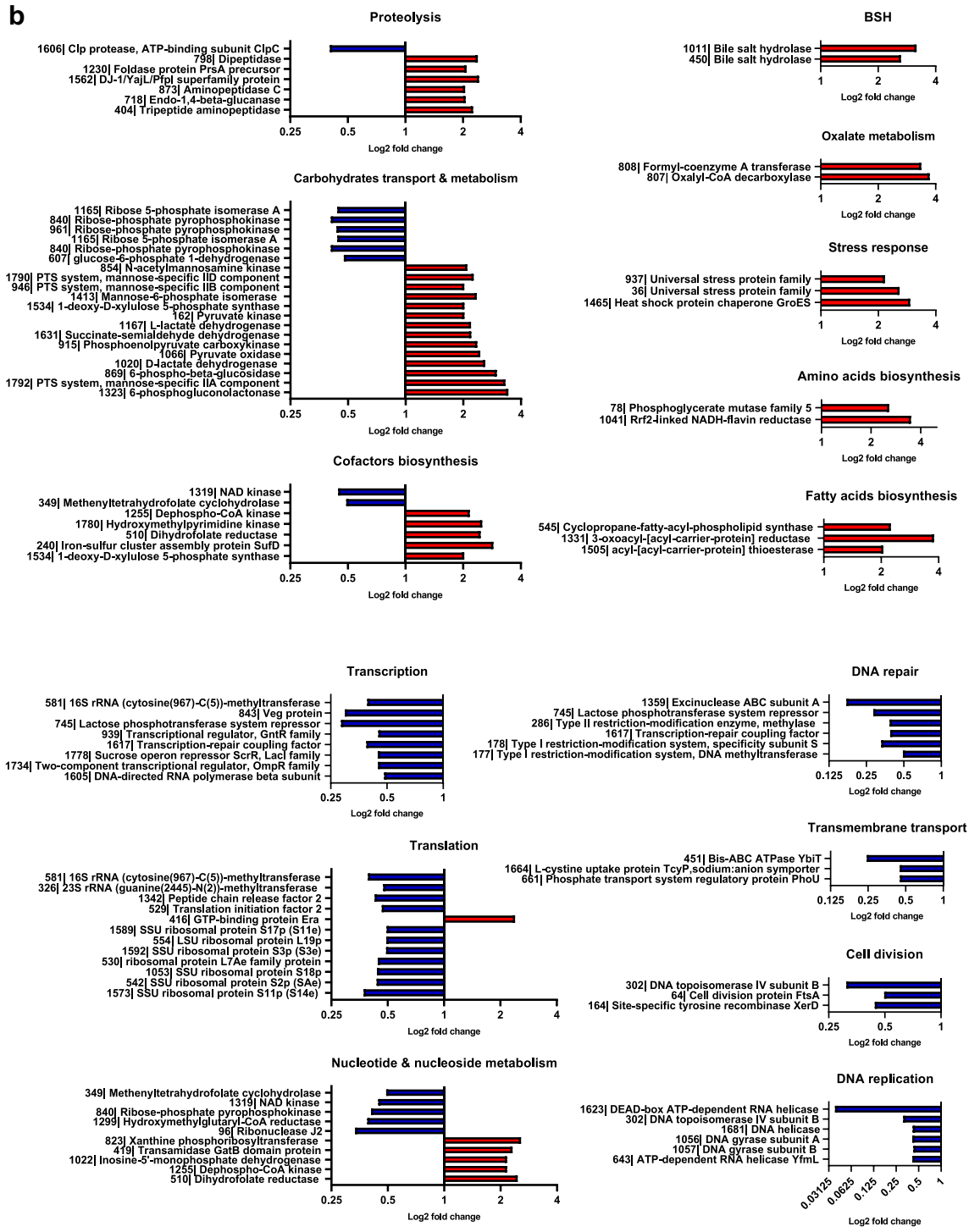

Figure 9. (Continued).

folate and iron-sulfur (Fe-S) cluster biosynthesis. In contrast, M11 showed a significant downregulation of proteins involved in transcription and transcriptional regulation, including 48 ribosomal proteins and the mutated S21p protein. Other downregulated proteins were involved in transmembrane transport, translation, DNA replication, cell division and DNA and protein repair.

In the stationary growth phase, most of the altered functions were similar to those observed in exponential growth phase. In addition, M11 samples also showed a higher abundance of

proteins involved in general stress response and fatty acid and amino acid biosynthesis compared to wild-type samples. Interestingly, the mutated GtrA protein showed no difference in abundance between M11 and wild-type in either growth phases assays.

*In vivo anti-*Giardia *activity*

The anti-*Giardia* activity of *L. johnsonii* CNCM I-4884 wild-type and M11 were investigated *in vivo* in a murine model of giardiasis. Five-days-old OF1 mice were treated daily by probiotic gavage for 10 d and challenged with *G. intestinalis* trophozoites 5 d after the first probiotic administration. Six days after infection, *G. intestinalis* trophozoites were quantified in the small intestine (Figure 10). Both probiotic treatments significantly reduced trophozoite load compared to PBS control. In addition, M11 enhanced trophozoites growth inhibition compared to wild-type, with a respective reduction of parasite load of 43.8% and 64.4% compared to PBS control. As BSH activity could affect weight gain in young animals,[58] we monitored daily weight gain; however, no difference was observed between mice receiving probiotic treatments compared with control mice (data not shown).

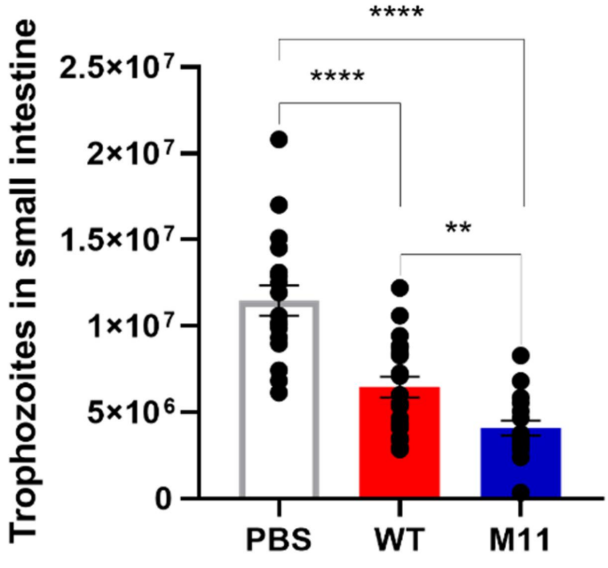

Figure 10. Reduction of *G. intestinalis* trophozoite load in the small intestine of OF1 mice treated daily with either PBS, *L. johnsonii* CNCM I-4884 wild-type or M11, 6 d after *Giardia* infection challenge. Values are mean ± SEM (n=18). Asterisks indicate statistical significance, as determined with unpaired t-test (****p<0.0001; **p<0.01).

Materials and methods

Bacterial strains

Lactobacillus johnsonii CNCM I-4884 wild type and its derivatives (M1 to M12) as well as *Lacticaseibacillus rhamnosus* strain GG (LGG, ATCC 53103) were stored at −80°C in Man Rogosa Sharpe (MRS) broth (Difco, France) with 20% glycerol until further analysis. Strains were routinely grown in MRS at 37°C under microaerobic conditions.

Intestinal cell lines

The human colon adenocarcinoma cell lines Caco-2 and HT-29 were obtained from the American Type Tissue Collection (ATCC® HTB-37™ and ATCC® HTB-38™ respectively), the T84 cell line was obtained from the European Collection of Authenticated Cell Cultures (ECACC 88021101), and the mucus-producing HT-29 MTX cell line was obtained from the Sloan Kettering Memorial Cancer Center (SKMCC). All cell lines were grown in Dulbecco modified Eagle's medium (DMEM) supplemented with 1% penicillin/streptomycin and 20%, 10%, 10% and 6% heat-inactivated fetal calf serum (FCS), respectively. The culture medium of Caco-2 cells was supplemented with 1% non-essential amino acids. Cell lines were maintained at 37°C in a humidified atmosphere with 10% CO_2.

Selection of stress-resistant derivatives of L. johnsonii *CNCM I-4884*

Resistance to free BAs

Overnight cultures of isolated clones of *L. johnsonii* CNCM I-4884 were streaked on MRS agar plates with a gradient (from 0 up to 1 mg/ml) of free BAs (mix of cholic acid and deoxycholic acid, Sigma, USA) and incubated at 37°C under anaerobic conditions. After 48 h, clones with the highest resistance were streaked successively on MRS agar plates with gradients of free BAs up to 2 mg/ml and 3 mg/ml. Clones obtained after the third passage were considered resistant to these BAs.

Resistance to autolysis

Mutants with altered sedimentation profiles were isolated using Todd Hewitt broth supplemented with 0.5% yeast extract (THY) with a low agar concentration (0.03%) as previously described.[32] Fifty ml flasks of THY semi-liquid medium were inoculated with 10 µl of a diluted *L. johnsonii* CNCM I-4884 overnight culture, corresponding to approximately 5 to 10 cells/flask, and incubated at 37°C for 14 d until appearance of slow sedimenting clones (see Figure 1d). Clones with different sedimentation profiles were then isolated on MRS agar plates. Overnight cultures of the recovered clones were washed twice in Phosphate Buffered Saline (PBS), diluted to an optical density at 600 nm (OD_{600}) = 0.7 in 50 mM K_2HPO_4/KH_2PO_4 pH 7 + 0.05% Triton X-100 (Merck, Germany) and incubated at 37°C. Lysis was monitored by measuring the decrease in OD_{600} in the cell suspensions.

Resistance to conjugated BAs

Overnight cultures of clones resistant to autolysis and free BAs were streaked on MRS agar plates with a gradient (from 0 up to 10 mg/ml) of conjugated BAs (mix of sodium taurodeoxycholate and sodium glycodeoxycholate, Sigma, USA) and incubated at 37°C under anaerobic conditions. Clones obtained after the last screening were considered resistant to these BAs.

*In vitro anti-*Giardia *activity*

The anti-*Giardia* activity of *L. johnsonii* CNCM I-4884 wild-type and derivatives was assessed as previously described.[31] Briefly, bacterial strains were grown in modified Keiser's TYI-S-33 (KM) medium supplemented with 10% FCS for 20 h under anaerobic conditions. Filtered bacterial supernatants were co-incubated with *G. intestinalis* WB6 trophozoites at 1.33×10^5 cells/ml in KM at pH 6.0 supplemented with 10% FCS and 0.6 mg/ml bovine bile at a volumetric ratio of 1:3 at 37°C under anaerobic conditions. After 22 h, samples were ice-chilled for 10 min and trophozoite load was determined using hemocytometer (flagellar mobility was used to assess parasite viability).

Adhesion to intestinal cell lines

Caco-2, HT-29, HT-29 MTX and T84 cells were seeded at 1×10^5 cells/well in 24-well culture plates and grown for 21 d. Antibiotics were removed from the culture medium 24 h prior to co-incubation with bacteria. Overnight bacterial cultures were washed twice with PBS and resuspended in antibiotic-free cell culture medium and added to each well at 2×10^8 CFU/ml. After 1 h incubation, cells were washed twice with PBS, adherent bacteria were detached from the cells using 0.05% Triton X-100 (Merck, Germany) and enumerated on MRS agar plates. The results are expressed as the percentage of bacteria adhering to the intestinal cells. LGG strain was used as a positive control.

Biofilm formation

Overnight cultures of *L. johnsonii* CNCM I-4884 wild-type and derivatives were used to inoculate MRS in 96-well microplates (1:100). Bacteria adhered for 1 h at 37°C and were then washed twice with fresh medium. After 24 h incubation at 37°C, the obtained biofilms were stained with SYTO 9 (Life Technologies). After 30 min incubation, images were acquired with a Leica SP8 confocal laser scanning microscope (CLSM, Leica Microsystems). The emitted fluorescence signal was collected on a hybrid detector in the 500–550 nm range after excitation at 488 nm with an Argon laser set at 20% of its maximum intensity with a z-step of 1 µm and at 600 hz. Simulated 3D fluorescence projections were generated using IMARIS 9.1 software and biomass was calculated from raw images using Eclipse software.

Transmission electron microscopy (TEM)

Exponential cultures of *L. johnsonii* CNCM I-4884 wild-type and derivatives were washed twice with PBS and fixed with 2% glutaraldehyde in 0.1 M sodium cacodylate buffer at pH 7.2 for 1 h at room temperature. The samples were then counterstained and analyzed as described in.[59]

BSHs activity

L. johnsonii CNCM I-4884 wild-type and derivatives were cultured in KM medium adjusted to pH 6.0 and supplemented with 10% FCS for 8 h at 37°C under anaerobic conditions. BA concentrations were measured by HPLC-MS/MS as previously described.[60] Experiments were stopped at various time points (0, 15, 30, 60, and 120 min) for each sample. We utilized a Sciex 5500Q-Trap mass spectrometer coupled with a Shimadzu LC-20ADXR dual binary flow HPLC system and a Kinetex 5 µm, 100 × 2.1 mm, C18 100 Å column (Phenomenex). Direct enzymatic activities were assessed by observing the decrease in conjugated BAs and the corresponding increase in unconjugated BAs.

Whole genome sequencing and identification of mutations

Genomic DNA extraction, sequencing, and annotation were carried out as previously described.[37] The genomes of M3, M5 and M11 derivatives were compared to the wild-type genome using the PATRIC variation analysis service. For each mutant strain, Illumina reads were mapped directly against the reference wild-type genome sequence using the BWA-MEM strict aligner. Single nucleotide polymorphisms (SNPs) and short insertions or deletions were identified using the FreeBayes method, and the effects of these SNPs were predicted with SNPeff.

Proteomic analysis

Protein extraction

Cell pellets from exponential and stationary cultures of *L. johnsonii* CNCM I-4884 wild-type and M11 were resuspended in PBS supplemented with protease inhibitor (Roche, Germany). After homogenization with 0.10 to 0.25 mm diameter glass beads (Fisher Scientific) using a Precellys Evolution homogenizer (Bertin Technologies, France) for 3 × 30 s at 6,400 rpm, the suspensions were centrifuged for 5 min at 13,000 g and the supernatants were collected. Ten mg of each protein extract were separated by a short migration in a polyacrylamide gel. Gel pieces with total protein extracts were collected and incubated with 10 mm DTT at 56°C for 30 min. Samples were then supplemented with 55 mm iodoacetamide and incubated in the dark at room temperature for 45 min (alkylation). Subsequently, 50 mm NH_4CO_3 and 50% acetonitrile (ACN) were added to each sample. After 15 min, gel pieces were incubated with 100% ACN. Next, liquid was removed and 100 ng trypsin (Promega) was added, and samples were incubated first at 4°C for 15 min and then overnight at 37°C. Samples were first incubated with 50 mm NH_4CO_3 for 10 min, followed by 15 min incubation with 0.5% trifluoroacetic acid (TFA) and 50% ACN. Samples were then dried and resuspended in 0.08% TFA and 2% ACN.

LC-MS/MS analysis

The LC-MS/MS method was adapted from.[61] MS analyses were performed on a Dionex U3000 RSLC coupled to an Orbitrap Fusion™ Lumos™ Tribrid™ mass spectrometer (Thermo Fisher Scientific). A 2 µl sample was loaded at 20 µl/min on a precolumn (µ-Precolumn, 300 µm i.d × 5 mm, C18 PepMap100, 5 µm, 100 Å, Thermo Fisher) and washed with loading buffer. After 3 min, the precolumn cartridge was connected to the separating column (Acclaim PepMap®, 75 µm × 500 mm, C18, 2 µm, 100 Å, Thermo Fisher). Buffer A consisted of 0.1% formic acid in 2% acetonitrile and buffer B of 0.1% formic acid in 80% acetonitrile. The gradient was executed at 250 nl/min with a linear gradient from 2% to 40% of buffer B for 115 min, and one run took 147 min including the generation phase (98% of buffer B). LC-MS/MS analysis was performed utilizing a nanospray ionization source and the eluted peptides were ionized by applying 1,6 kV in positive mode. MS scans were performed at 120,000 resolution, m/z range 400–1,500 Da. MS/MS analysis was performed in a data-dependent mode, with a top speed cycle of 3 s for the most intense double or multiple charged precursor ions. Ions in each MS scan over threshold 50,000 were selected for fragmentation (MS2) by higher energy collisional dissociation (HCD) at 30% for identification and detection in the orbitrap followed by top speed MS2 fragment ions. Precursors were isolated in the quadrupole with a 1.2 m/z window and dynamic exclusion within 10 ppm during 80 s was used for m/z-values already

selected for fragmentation. The AGC targets were fixed as custom and standard for MS and MS/MS, respectively.

Proteins identification and quantification

A FASTA format database was used from *L. johnsonii* CNCM I-4884 WT genome (1809 entries,[37]). A database of common contaminants was also used for the analysis. Database searches were performed using the i2MassChroQ (version 0.4.62, http://pappso.inrae.fr/) with one possible missed cleavage. Carboxyamidomethylation of cysteine residues and oxidation of methionine residues were set to "static" and "possible" modifications, respectively. Precursor and fragment mass tolerance was 10 ppm. Identified proteins were filtered and grouped using i2MassChroQ. Data filtering was achieved according to a peptide *E*-value <0.01, protein log (E-value) < −4 and to a minimum of two identified peptides per protein. Relative quantification of protein abundances was performed using extracted ion chromatograms (XIC) method defined as the sum of MS1 intensities of all peptides associated with a protein. Data post-processing and statistical analysis were performed by using the R package4 MCQR 0.4.3 as previously described.[62]

*In vivo anti-*Giardia *activity*

The anti-*Giardia* activity of *L. johnsonii* CNCM I-4884 wild-type and M11 was investigated *in vivo* as previously described.[31] Bacterial strains (5×10^8 CFU in PBS with 15% glycerol) were administered daily by intragastric gavage to 5 d old OF1 mice (Charles River, France) for 10 d. Control animals received PBS with 15% glycerol. Mice were then challenged with 1×10^5 *G. intestinalis* WB6 trophozoites at 10 d of age by intragastric gavage. Mice were euthanized by cervical dislocation at 16 d of age. The small intestine was opened, resuspended in 5 ml ice-chilled PBS and mixed thoroughly. Trophozoites were enumerated using a hemocytometer. Protocols were conducted in accordance with the institutional guidelines approved by the local ethical committee and the Ministère de l'Education Nationale, de l'Enseignement Supérieur et de la Recherche, France (APAFIS #37444–2022050516561397).

Statistical analysis

Statistical differences were determined using ANOVA and unpaired *t*-tests. All statistics were performed using GraphPad Prism (version 9.00) and values of p less than 0.05 were considered to be statistically significant.

Discussion

In this study, we employed an adaptive evolution strategy to generate stress-resistant derivatives of *L. johnsonii* CNCM I-4884, with the aim of improving both BSH production and anti-*Giardia* activity in the strain. Adaptive evolution has been widely used to generate strains with phenotypes-of-interest, such as improved production of metabolites, like gamma-aminobutyric acid[63] as well as enhanced tolerance to acid stress,[64,65] temperature,[66] antibiotic,[67] or high NaCl concentrations.[68] Here, this approach generated a collection of 12 stress-resistant derivatives, which were further evaluated at phenotypic and genetic levels. The candidate M11 showed the most marked phenotype, with a significantly improved anti-*Giardia* activity *in vitro* correlated with improved BSH activity toward two types of conjugated BAs. Although adaptive evolution has proven to be highly effective, it may result in significant genome rearrangements, including large deletions previously reported.[66] Here, the presence of mutations affecting a single nucleotide was confirmed by whole genome sequencing. Two SNPs were identified in M11 genome relative to wild-type strain. The first mutation was identified in a gene encoding a putative flippase with homology to the GtrA superfamily involved in EPS biosynthesis. The reduced expression of EPS may be responsible for the enhanced auto-aggregative phenotype and adhesion to intestinal epithelial cell lines of M11, conferring the mutant a selective advantage for GIT colonization.[53–55] Modifications in cell wall structure have been previously described in other laboratory adapted strains in the presence of stress.[69,70] A second mutation was identified in *rpsU* gene encoding the 30S small subunit ribosomal protein S21p. Variants of *L. monocytogenes* mutated in the *rpsU* gene showed upregulation of the general stress factor Sigma B and SigB regulon

members which are associated with a stress-resistant phenotype.[71] Through proteomic analysis, we identified a number of differentially expressed proteins in M11 compared to wild-type. Similar to what has been observed in *L. monocytogenes* variants, SigB was significantly increased in M11 compared to wild-type, with 2.38 and 2.20 log2 fold change in exponential and stationary growth phases, respectively. This result suggests that the upregulation of general stress response by SigB may be responsible for M11 improved BAs resistance. The activation of a systemic stress defense response via SigB is energetically costly, resulting in a negative impact on growth. Indeed, M11 showed an altered growth rate compared to wild-type in standard conditions. However, when cultured in the presence of BAs, the growth of M11 was significantly improved, indicating a trade-off between stress resistance and fitness, as observed in previous studies.[65,71,72] The impaired growth rate of M11 may also be attributed to the competition between SigB and housekeeping SigA for the RNA polymerase, with the latter responsible for the transcription of growth-related genes.[71] Moreover, the activation of SigB may be responsible for the enhanced biofilm formation of M11, as reported in *L. monocytogenes*[73] and *B. subtilis*.[74]

Furthermore, the comparative analysis of M11 and wild-type proteomes revealed a higher abundance of proteins involved in glycolysis, the pentose phosphate pathway and pyruvate metabolism. Previous studies have reported up-regulation of these pathways in other *Lactobacillus* species in response to acid stress[75–78] and bile stress.[79–84] This has been showed to result in increased ATP production, thereby providing the strain with sufficient energy to meet the elevated energy demands and the stress associated with the adaptation to BAs. The overexpression of L- and D-lactate dehydrogenase resulted in increased lactate and ATP production, as well as NAD+ regeneration, which collectively maintained redox balance during BAs stress. M11 also presented an increased abundance of formyl-CoA transferase and oxalyl-CoA carboxylase, involved in oxalate metabolism. This could represent an alternative energy source in the absence or depletion of a carbohydrate source[85] and is important for bile stress resistance and GIT colonization.[82,86] M11 also showed an enrichment of proteins with predicted peptidase activity. The overexpression of the proteolytic system is commonly observed in lactobacilli in response to acid and bile stress, in order to provide amino acids for the synthesis and repair of proteins damaged by stress.[78,81,87,88] In addition, M11 exhibited a greater abundance of proteins involved in co-factor biosynthesis, particularly the SUF machinery responsible for the assembly of Fe-S clusters. These clusters are essential for the correct activity of housekeeping proteins and transcriptional regulators under stress conditions.[89] A role of the SUF machinery has been also described in stress resistance and biofilm formation.[90] In addition, M11 overexpressed proteins with oxidoreductase activity, which is consistent with previous studies.[81,83] In addition to improving tolerance to bile-induced oxidative stress, the NADH-dependent oxidoreductase results in the recycling of ATP and doubles the ATP yield from carbohydrate metabolism, thereby amplifying the energy generation.[79]

Of particular interest is the overexpression of BSH450 and BSH1011 in M11 compared to wild-type. These findings are corroborated by the increased deconjugated activity of the M11 mutant toward both tauro- and glyco-conjugated substrates. These results align with a previous transcriptomic study which reported increased *bsh* expression in a variant of *L. monocytogenes* inactivated in *rpsU* gene.[55] Moreover, additional research has indicated that the overexpression of BSH enzymes in response to bile stress has a favorable impact on adhesion and GIT persistence in other *Lactobacillus* species.[82,87,91,92]

The majority of down-regulated proteins in M11 are involved in cell division, DNA replication, transcription and translation, which is consistent with the decreased growth rate of M11 compared to wild-type observed in MRS medium. Surprisingly, proteins with chaperone activity and ABC transporters were also less abundant in M11 relative to wild-type. These findings contradict previous studies reporting an increase of these activities in response to stress in several *Lactobacillus* species, as they play an important role in the recycling of damaged proteins and the efflux of bile stress-related compounds.[80,87,88,93–95]

In stationary phase, M11 samples showed a further increase in proteins involved in the

biosynthesis of unsaturated and cyclopropane fatty acids (CFA). Previous studies have reported increased CFA biosynthesis in lactobacilli in response to bile stress, preserving membrane integrity and counteracting proton influx.[93,95–97] As described for other *Lactobacillus* species in response to stress, proteins involved in serine and lysine biosynthesis are more abundant in M11 compared to wild-type.[75,84,87,98] It has been suggested that the increased lysine biosynthesis may facilitate lysinylation of membrane lipids and thus improve stress-resistance by altering the surface charge to repulse cationic bile compounds.[84,87] Furthermore, M11 displayed increased abundance of universal stress proteins, consistent with previous observations in response to stress.[75,79,81] It was also found that the universal stress protein UspA was upregulated in M11 strain. Of note, this protein has been reported to play a role in biofilm formation, and may be responsible for the enhanced biofilm biovolume of M11.[99,100]

Finally, the inhibitory activity of M11 was investigated *in vivo* in a suckling murine model of giardiasis. Mice treated with M11 exhibited a significantly higher reduction in parasite burden in the small intestine compared to those treated with wild-type, confirming the results observed *in vitro* on *Giardia* trophozoites. These findings substantiated the correlation between increased BSH activity and increased anti-*Giardia* activity both *in vitro* and *in vivo*.

A potential limitation of this study is the absence of complemented strains to confirm the role of RpsU in stress resistance and BSH activities. The whole genome sequencing of M11 helps to mitigate this limitation as it provides the complete genetic context of the mutations. Another limitation of this study is the absence of a negative control in the murine experiment. Further studies could benefit from the addition of a treatment group with a non BSH-producing strain or the administration of BSH inhibitors[101,102] in order to confirm the role of these enzymes in the anti-*Giardia* activity of the strains.

In conclusion, this work provides evidence that adaptative evolution, resulting in the incorporation of single amino acid substitutions in GrtA and RpsU, has enhanced the stress-resistance, BSH production and consequently anti-*Giardia* activity of *L. johnsonii* CNCM I-4884 both *in vitro* and *in vivo*. Overall, our study describes an evolutive approach to develop more robust food-grade derivatives from wild-type probiotic strains, significantly enhancing their beneficial properties.

Acknowledgments

This work has benefited from the facilities and expertise of MIMA2, INRAE. Microscopy and Imaging Facility for Microbes, Animals and Foods, https://doi.org/10.15454/1.5572348210007727E12. Proteomics analyses were performed on the PAPPSO platform (http://pappso.inra.fr.) which is supported by INRAE (http://www.inrae.fr.), the Ile-de-France regional council (https://www.iledefrance.fr/education-recherche.), IBiSA (https://www.ibisa.net.) and CNRS (http://www.cnrs.fr).

Disclosure statement

The authors declare that A. S. B. received a salary from Boehringer Ingelheim Animal Health, as part of a CIFRE PhD contract. H.R. and M.G. are currently employees of Boehringer Ingelheim Animal Health. The other authors declare no competing interests.

Funding

This research was funded by Boehringer Ingelheim, Association Nationale de la Recherche et de la Technologie [ANRT 2019/0369] and Agence Nationale de la Recherche [ANR-23-CE18-0022].

ORCID

Anne-Sophie Boucard http://orcid.org/0000-0002-8109-0954
Céline Henry http://orcid.org/0000-0002-2355-1791
Isabelle Florent http://orcid.org/0000-0002-7140-6417

Authors' contributions

Conceptualization, L.G.B.-H., I.F., and B.P.; methodology, A.-S.B., S.K., L.G.B.-H., B.P. and I.F.; software, A.-S.B.; A.M.-O., C.M., C.H. and C.P.; validation, L.G.B.-H., S.K.; B.P. and I.F.; formal analysis, A.-S.B., S.K., L.G.B.-H.; investigation, A.-S.B., J.A., S.C. and M.M.; resources, B.P., I.F. and L.G.B.-H.; data curation, A.-S.B. and L.G.B.-H.; writing-original draft preparation, A.-S.B. and L.G.B.-H.; writing-review and editing, A.-S.B., H.R., M.G., P.L., B.P., I.F. and L.G.B.-H.; supervision, L.G.B.-H., B.P. and I.F.; project administration, L.G.B.-H.; funding acquisition, L.G.B.-H., I.F., and B.P. All authors have read and agreed to the published version of the manuscript.

References

1. Cernikova L, Faso C, Hehl AB, Odom AR. Five facts about *Giardia lamblia*. PLOS Pathog. 2018;14(9): e1007250. doi:10.1371/journal.ppat.1007250.
2. Litleskare S, Wensaas K-A, Eide GE, Hanevik K, Kahrs GE, Langeland N, Rortveit G. Perceived food intolerance and irritable bowel syndrome in a population 3 years after a giardiasis-outbreak: a historical cohort study. BMC Gastroenterol. 2015;15 (1):164. doi:10.1186/s12876-015-0393-0.
3. Nakao JH, Collier SA, Gargano JW. Giardiasis and subsequent irritable bowel syndrome: a longitudinal cohort study using health insurance data. J Infect Dis. 2017;215(5):798–805. doi:10.1093/infdis/jiw621.
4. Rogawski ET, Liu J, Platts-Mills JA, Kabir F, Lertsethtakarn P, Siguas M, Khan SS, Praharaj I, Murei A, Nshama R, et al. Use of quantitative molecular diagnostic methods to investigate the effect of enteropathogen infections on linear growth in children in low-resource settings: longitudinal analysis of results from the MAL-ED cohort study. Lancet Glob Health. 2018;6(12):e1319–e1328. doi:10.1016/S2214-109X(18)30351-6.
5. Argüello-García R, Leitsch D, Skinner-Adams T, Ortega-Pierres MG. Advances in parasitology. Drug resistance in Giardia: mechanisms and alternative treatments for Giardiasis. 2020;107:201–282. doi: 10.1016/bs.apar.2019.11.003
6. Lalle M, Hanevik K. Treatment-Refractory Giardiasis: challenges and solutions. Infect Drug Resist. 2018;11:1921–1933. doi:10.2147/IDR.S141468.
7. Mørch K, Hanevik K. Giardiasis treatment: an update with a focus on refractory disease. Curr Opin Infect Dis. 2020;33(5):355–364. doi:10.1097/QCO.0000000000000668.
8. Riches A, Hart CJS, Trenholme KR, Skinner-Adams TS. Anti- *Giardia* drug discovery: current status and gut feelings. J Med Chem. 2020;63(22):13330–13354. doi:10.1021/acs.jmedchem.0c00910.
9. Calzada F, Bautista E. Plants used for the treatment of diarrhoea from Mexican Flora with amoebicidal and giadicidal activity, and their phytochemical constituents. J Ethnopharmacol. 2020;253:112676. doi:10.1016/j.jep.2020.112676.
10. Dyab AK, Yones DA, Ibraheim ZZ, Hassan TM. Anti-giardial therapeutic potential of dichloromethane extracts of Zingiber officinale and *Curcuma longa* in vitro and in vivo. Parasitol Res. 2016;115 (7):2637–2645. doi:10.1007/s00436-016-5010-9.
11. Asfaram S, Fakhar M, Keighobadi M, Akhtari J. Promising anti-protozoan activities of propolis (bee glue) as natural product: a review. Acta Parasitol. 2021;66(1):1–12. doi:10.1007/s11686-020-00254-7.
12. Frontera LS, Moyano S, Quassollo G, Lanfredi-Rangel A, Rópolo AS, Touz MC. Lactoferrin and lactoferricin endocytosis halt *Giardia* cell growth and prevent infective cyst production. Sci Rep. 2018;8(1):18020. doi:10.1038/s41598-018-36563-1.
13. Keselman A, Li E, Maloney J, Singer SM, Young VB. The microbiota contributes to CD8 $^{+}$ T cell activation and nutrient malabsorption following intestinal infection with *Giardia duodenalis*. Infect Immun. 2016;84 (10):2853–2860. doi:10.1128/IAI.00348-16.
14. Singer SM, Nash TE. The role of Normal Flora in *Giardia lamblia* infections in mice. J Infect Dis. 2000;181(4):1510–1512. doi:10.1086/315409.
15. Hill C, Guarner F, Reid G, Gibson GR, Merenstein DJ, Pot B, Morelli L, Canani RB, Flint HJ, Salminen S, et al. The international scientific association for probiotics and prebiotics consensus statement on the scope and appropriate use of the term probiotic. Nat Rev Gastroenterol Hepatol. 2014;11(8):506–514. doi:10.1038/nrgastro.2014.66.
16. Ishaque SM, Khosruzzaman SM, Ahmed DS, Sah MP. A randomized placebo-controlled clinical trial of a multi-Strain Probiotic formulation (bio-Kult®) in the management of diarrhea-predominant irritable bowel syndrome. BMC Gastroenterol. 2018;18(1):71. doi:10.1186/s12876-018-0788-9.
17. Bjarnason I, Sission G, Hayee B. A randomised, double-blind, placebo-controlled trial of a multi-strain probiotic in patients with asymptomatic ulcerative colitis and Crohn's disease. Inflammopharmacology. 2019;27 (3):465–473. doi:10.1007/s10787-019-00595-4.
18. Kassaian N, Feizi A, Aminorroaya A, Amini M. Probiotic and synbiotic supplementation could improve metabolic syndrome in prediabetic adults: a randomized controlled trial. Diabetes Metab Syndr Clin Res Rev. 2019;13(5):2991–2996. doi:10.1016/j.dsx.2018.07.016.
19. Gutiérrez-Castrellón P, Gandara-Martí T, Abreu Y Abreu AT, Nieto-Rufino CD, López-Orduña E, Jiménez-Escobar I, Jiménez-Gutiérrez C, López-Velazquez G, Espadaler-Mazo J. Probiotic improves symptomatic and viral clearance in COVID-19 outpatients: a randomized, quadruple-blinded, placebo-controlled trial. Gut Microbes. 2022;14(1):2018899. doi:10.1080/19490976.2021.2018899.
20. Perrucci S, Fichi G, Ricci E, Galosi L, Lalle M, Rossi G, Giuffrè A. In vitro and ex vivo evaluation of the anti-giardia duodenalis activity of the supernatant of Slab51 (SivoMixx). PLOS ONE. 2019;14(3):e0213385. doi:10.1371/journal.pone.0213385.
21. Fonseca JF, Alvim LB, Nunes ÁC, Oliveira FMS, Amaral RS, Caliari MV, Nicoli JR, Neumann E, Gomes MA. Probiotic effect of Bifidobacterium Longum 5 ^{1A} and Weissella Paramesenteroides WpK4 on gerbils infected with *Giardia lamblia*. J Appl Microbiol. 2019;127(4):1184–1191. doi:10.1111/jam.14338.
22. Shukla G, Devi P, Sehgal R. Effect of *lactobacillus casei* as a probiotic on modulation of giardiasis. Dig Dis Sci. 2008;53(10):2671–2679. doi:10.1007/s10620-007-0197-3.

23. Hassan ZR, Salama DEA, Ibrahim HF, Ahmed SG. Ultrastructural changes and IgA modulatory effect of commercial prebiotic and probiotic in murine giardiasis. J Parasit Dis Off Organ Indian Soc Parasitol. 2023;47(2):224–237. doi:10.1007/s12639-022-01552-9.
24. Fenimore A, Martin L, Lappin MR. Evaluation of metronidazole with and without enterococcus faecium SF68 in shelter dogs with diarrhea. Top Companion Anim Med. 2017;32(3):100–103. doi:10.1053/j.tcam.2017.11.001.
25. Besirbellioglu BA, Ulcay A, Can M, Erdem H, Tanyuksel M, Avci IY, Araz E, Pahsa A. Saccharomyces Boulardii and infection due to *Giardia lamblia*. Scand J Infect Dis. 2006;38(6–7):479–481. doi:10.1080/00365540600561769.
26. Benyacoub J, Pérez PF, Rochat F, Saudan KY, Reuteler G, Antille N, Humen M, De Antoni GL, Cavadini C, Blum S, et al. Enterococcus Faecium SF68 enhances the immune response to giardia intestinalis in mice. J Nutr. 2005;135(5):1171–1176. doi:10.1093/jn/135.5.1171.
27. Shukla G, Kamboj S, Sharma B. Comparative analysis of antigiardial potential of heat inactivated and probiotic protein of probiotic lactobacillus rhamnosus GG in murine giardiasis. Probiotics Antimicrob Proteins. 2020;12(1):271–279. doi:10.1007/s12602-018-9506-8.
28. Shukla G, Sharma A, Bhatia R, Sharma M. Prophylactic potential of synbiotic (*Lactobacillus casei* and inulin) in malnourished murine giardiasis: an immunological and ultrastructural study. Probiotics Antimicrob Proteins. 2019;11(1):165–174. doi:10.1007/s12602-017-9368-5.
29. Amer EI, Mossallam SF, Mahrous H. Therapeutic enhancement of newly derived bacteriocins against Giardia lamblia. Exp Parasitol. 2014;146:52–63. doi:10.1016/j.exppara.2014.09.005.
30. Ribeiro MRS, Oliveira DR, Oliveira FMS, Caliari MV, Martins FS, Nicoli JR, Torres MF, Andrade MER, Cardoso VN, Gomes MA. Effect of Probiotic Saccharomyces Boulardii in Experimental Giardiasis. Benef Microbes. 2018;9(5):789–798. doi:10.3920/BM2017.0155.
31. Allain T, Chaouch S, Thomas M, Travers M-A, Valle I, Langella P, Grellier P, Polack B, Florent I, Bermúdez-Humarán LG. Bile salt hydrolase activities: a novel target to screen Anti-Giardia Lactobacilli? Front Microbiol. 2018;9:89. doi:10.3389/fmicb.2018.00089.
32. Couvigny B, Kulakauskas S, Pons N, Quinquis B, Abraham A-L, Meylheuc T, Delorme C, Renault P, Briandet R, Lapaque N, et al. Identification of new factors modulating adhesion abilities of the pioneer commensal bacterium streptococcus salivarius. Front Microbiol. 2018;9:273. doi:10.3389/fmicb.2018.00273.
33. Motta J-P, Wallace JL, Buret AG, Deraison C, Vergnolle N. Gastrointestinal biofilms in health and disease. Nat Rev Gastroenterol Hepatol. 2021;18(5):314–334. doi:10.1038/s41575-020-00397-y.
34. Aoudia N, Rieu A, Briandet R, Deschamps J, Chluba J, Jego G, Garrido C, Guzzo J. Biofilms of Lactobacillus Plantarum: And Lactobacillus Fermentum: Effect On Stress Responses, Antagonistic Eff On Pathogen Growth And Immunomodulatory Prop. Food Microbiol. 2016;53:51–59. doi:10.1016/j.fm.2015.04.009.
35. Heumann A, Assifaoui A, Da Silva Barreira D, Thomas C, Briandet R, Laurent J, Beney L, Lapaquette P, Guzzo J, Rieu A. Intestinal release of biofilm-like microcolonies encased in calcium-pectinate beads increases probiotic properties of Lacticaseibacillus Paracasei. Npj Biofilms Microbiomes. 2020;6(1):44. doi:10.1038/s41522-020-00159-3.
36. Wang X, Cao Z, Zhang M, Meng L, Ming Z, Liu J. Bioinspired oral delivery of gut microbiota by self-coating with biofilms. Sci Adv. 2020;6(26):eabb1952. doi:10.1126/sciadv.abb1952.
37. Boucard A-S, Florent I, Polack B, Langella P, Bermúdez-Humarán LG. Genome sequence and assessment of safety and potential probiotic traits of Lactobacillus Johnsonii CNCM I-4884. Microorganisms. 2022;10(2):273. doi:10.3390/microorganisms10020273.
38. Bittner L-M, Arends J, Narberhaus FW. When, how and why? Regulated proteolysis by the essential FtsH protease in Escherichia Coli. Biol Chem. 2017;398(5–-6):625–635. doi:10.1515/hsz-2016-0302.
39. Ito K, Akiyama Y. Cellular functions, mechanism of action, and regulation of FtsH protease. Annu Rev Microbiol. 2005;59(1):211–231. doi:10.1146/annurev.micro.59.030804.121316.
40. Langklotz S, Baumann U, Narberhaus F. Structure and function of the bacterial AAA protease FtsH. Biochim Biophys Acta BBA - Mol Cell Res. 2012;1823(1):40–48. doi:10.1016/j.bbamcr.2011.08.015.
41. Bron PA, Molenaar D, Vos WM, Kleerebezem M. DNA micro-array-based identification of bile-responsive genes in Lactobacillus Plantarum. J Appl Microbiol. 2006;100(4):728–738. doi:10.1111/j.1365-2672.2006.02891.x.
42. Bove P, Capozzi V, Garofalo C, Rieu A, Spano G, Fiocco D. Inactivation of the FtsH gene of lactobacillus plantarum WCFS1: effects on growth, stress tolerance, cell surface properties and biofilm formation. Microbiol Res. 2012;167(4):187–193. doi:10.1016/j.micres.2011.07.001.
43. Biswas S, Keightley A, Biswas I. Characterization of a stress tolerance-defective mutant of lactobacillus rhamnosus LRB. Mol Oral Microbiol. 2019;34(4):153–167. doi:10.1111/omi.12262.
44. Fiocco D, Collins M, Muscariello L, Hols P, Kleerebezem M, Msadek T, Spano G. The lactobacillus plantarum FtsH gene is a novel member of the CtsR stress response regulon. J Bacteriol. 2009;191(5):1688–1694. doi:10.1128/JB.01551-08.
45. Martínez B, Rodríguez A, Kulakauskas S, Chapot-Chartier M-P. Cell wall homeostasis in lactic acid

bacteria: threats and defences. FEMS Microbiol Rev. 2020;44(5):538–564. doi:10.1093/femsre/fuaa021.
46. Dominski Z, Carpousis AJ, Clouet-d'Orval B. Emergence of the β-casp Ribonucleases: highly conserved and ubiquitous metallo-enzymes involved in messenger RNA maturation and degradation. Biochim Biophys Acta BBA - Gene Regul Mech. 2013;1829(6––7):532–551. doi:10.1016/j.bbagrm.2013.01.010.
47. Even S. Ribonucleases J1 and J2: two novel endoribonucleases in B.Subtilis with functional homology to E. Coli RNase E. Nucleic Acids Res. 2005;33(7):2141–2152. doi:10.1093/nar/gki505.
48. Britton RA, Wen T, Schaefer L, Pellegrini O, Uicker WC, Mathy N, Tobin C, Daou R, Szyk J, Condon C. Maturation of the 5′ end of Bacillus Subtilis 16S rRNA by the essential ribonuclease YkqC/RNase J1. Mol Microbiol. 2007;63(1):127–138. doi:10.1111/j.1365-2958.2006.05499.x.
49. Claessen D, Emmins R, Hamoen LW, Daniel RA, Errington J, Edwards DH. Control of the cell elongation–division cycle by shuttling of PBP1 protein in Bacillus Subtilis. Mol Microbiol. 2008;68(4):1029–1046. doi:10.1111/j.1365-2958.2008.06210.x.
50. Haeusser DP, Schwartz RL, Smith AM, Oates ME, Levin PA. EzrA prevents aberrant cell division by modulating assembly of the cytoskeletal protein FtsZ: EzrA inhibits FtsZ assembly through direct interactions. Mol Microbiol. 2004;52(3):801–814. doi:10.1111/j.1365-2958.2004.04016.x.
51. Myrbråten IS, Wiull K, Salehian Z, Håvarstein LS, Straume D, Mathiesen G, Kjos M, Marco ML. CRISPR interference for rapid knockdown of essential cell cycle genes in Lactobacillus Plantarum. mSphere. 2019;4(2):e00007–19. doi:10.1128/mSphere.00007-19.
52. Mayer MJ, D'Amato A, Colquhoun IJ, Le Gall G, Narbad A, Cann I. Identification of genes required for glucan exopolysaccharide production in lactobacillus johnsonii suggests a novel biosynthesis mechanism. Appl Environ Microbiol. 2020;86(8). doi:10.1128/AEM.02808-19.
53. Dertli E, Mayer MJ, Narbad A. Impact of the Exopolysaccharide layer on Biofilms, adhesion and resistance to stress in lactobacillus johnsonii FI9785. BMC Microbiol. 2015;15(1):8. doi:10.1186/s12866-015-0347-2.
54. Jiang Y, Ren F, Liu S, Zhao L, Guo H, Hou C. Enhanced acid tolerance in Bifidobacterium Longum by adaptive evolution: comparison of the genes between the acid-resistant variant and wild-type strain. J Microbiol Biotechnol. 2016;26(3):452–460. doi:10.4014/jmb.1508.08030.
55. Denou E, Pridmore RD, Berger B, Panoff J-M, Arigoni F, Brüssow H. Identification of genes associated with the long-gut-persistence phenotype of the probiotic Lactobacillus Johnsonii strain NCC533 using a combination of genomics and transcriptome analysis. J Bacteriol. 2008;190(9):3161–3168. doi:10.1128/JB.01637-07.
56. Metselaar KI, den Besten HMW, Boekhorst J, van Hijum SAFT, Zwietering MH, Abee T. Diversity of acid stress resistant variants of listeria monocytogenes and the potential role of ribosomal protein S21 encoded by RpsU. Front Microbiol. 2015;6. doi:10.3389/fmicb.2015.00422.
57. Koomen J, den Besten HMW, Metselaar KI, Tempelaars MH, Wijnands LM, Zwietering MH, Abee T. Gene profiling-based phenotyping for identification of cellular parameters that contribute to fitness, stress-tolerance and virulence of listeria monocytogenes variants. Int J Food Microbiol. 2018;283:14–21. doi:10.1016/j.ijfoodmicro.2018.06.003.
58. Geng W, Lin J. Bacterial bile salt hydrolase: an intestinal microbiome target for enhanced animal health. Anim Health Res Rev. 2016;17(2):148–158. doi:10.1017/S1466252316000153.
59. Nicolas-Boluda A, Laurent G, Bazzi R, Roux S, Donnadieu E, Gazeau F. Two step promotion of a hot tumor immune environment by gold decorated iron oxide nanoflowers and light-triggered mild hyperthermia. Nanoscale. 2021;13(44):18483–18497. doi:10.1039/d1nr03201a.
60. Humbert L, Maubert MA, Wolf C, Duboc H, Mahé M, Farabos D, Seksik P, Mallet JM, Trugnan G, Masliah J, et al. Bile acid profiling in human biological samples: comparison of extraction procedures and application to normal and cholestatic patients. J Chromatogr B. 2012;899:135–145. doi:10.1016/j.jchromb.2012.05.015.
61. Millan-Oropeza A, Henry C, Lejeune C, David M, Virolle M-J. Expression of genes of the pho regulon is altered in Streptomyces Coelicolor. Sci Rep. 2020;10(1):8492. doi:10.1038/s41598-020-65087-w.
62. Bednarz B, Millan-Oropeza A, Kotowska M, Świat M, Quispe Haro JJ, Henry C, Pawlik K. Coelimycin synthesis activatory proteins are key regulators of specialized metabolism and precursor flux in Streptomyces Coelicolor A3(2). Front Microbiol. 2021;12(12):616050. doi:10.3389/fmicb.2021.616050.
63. Kim K, Hou CY, Choe D, Kang M, Cho S, Sung BH, Lee D-H, Lee S-G, Kang TJ, Cho B-K. Adaptive laboratory evolution of Escherichia Coli W enhances gamma-aminobutyric acid production using glycerol as the carbon source. Metab Eng. 2022;69:59–72. doi:10.1016/j.ymben.2021.11.004.
64. Du B, Olson CA, Sastry AV, Fang X, Phaneuf PV, Chen K, Wu M, Szubin R, Xu S, Gao Y, et al. Adaptive laboratory evolution of Escherichia Coli under acid stress. Microbiol Read Engl. 2020;166(2):141–148. doi:10.1099/mic.0.000867.
65. Han NR, Yu S, Byun JA, Yun EJ, Cheon S, Song S, Shim S, Choi I-G, Lee S-H, Kim KH. Evolution-aided improvement of the acid tolerance of Levilactobacillus Brevis and its application in sourdough fermentation.

Food Res Int Ott Ont. 2024;190:114584. doi:10.1016/j.foodres.2024.114584.
66. Oide S, Gunji W, Moteki Y, Yamamoto S, Suda M, Jojima T, Yukawa H, Inui M, Kivisaar M. Thermal and solvent stress cross-tolerance conferred to Corynebacterium Glutamicum by adaptive laboratory evolution. Appl Environ Microbiol. 2015;81(7):2284–2298. doi:10.1128/AEM.03973-14.
67. Sulaiman JE, Lam H, Bradford PA. Novel daptomycin tolerance and resistance mutations in methicillin-resistant Staphylococcus aureus from adaptive laboratory evolution. mSphere. 2021;6(5):e0069221. doi:10.1128/mSphere.00692-21.
68. Papadopoulou E, Rodriguez de Evgrafov MC, Kalea A, Tsapekos P, Angelidaki I. Adaptive laboratory evolution to hypersaline conditions of lactic acid bacteria isolated from seaweed. New Biotechnol. 2023;75:21–30. doi:10.1016/j.nbt.2023.03.001.
69. Conrad TM, Joyce AR, Applebee MK, Barrett CL, Xie B, Gao Y, Palsson BØ. Whole-genome resequencing of Escherichia Coli K-12 MG1655 undergoing short-term laboratory evolution in lactate minimal media reveals flexible selection of adaptive mutations. Genome Biol. 2009;10(10):R118. doi:10.1186/gb-2009-10-10-r118.
70. Kim YY, Kim J-C, Kim S, Yang JE, Kim HM, Park HW. Heterotypic stress-induced adaptive evolution enhances freeze-drying tolerance and storage stability of Leuconostoc Mesenteroides WiKim33. Food Res Int Ott Ont. 2024;175:113731. doi:10.1016/j.foodres.2023.113731.
71. Koomen J, Huijboom L, Ma X, Tempelaars MH, Boeren S, Zwietering MH, den Besten HMW, Abee T. Amino acid substitutions in ribosomal protein RpsU enable switching between high fitness and multiple-stress resistance in listeria monocytogenes. Int J Food Microbiol. 2021;351:109269. doi:10.1016/j.ijfoodmicro.2021.109269.
72. Ma X, Chen J, Zwietering MH, Abee T, Den Besten HMW. Stress resistant RpsU variants of listeria monocytogenes can become underrepresented due to enrichment bias. Int J Food Microbiol. 2024;416:110680. doi:10.1016/j.ijfoodmicro.2024.110680.
73. Dorey A, Marinho C, Piveteau P, O'Byrne C. Role and regulation of the stress activated sigma factor sigma B (ΣB) in the saprophytic and host-associated life stages of listeria monocytogenes. Adv Appl Microbiol. 2019;106:1–48. doi:10.1016/bs.aambs.2018.11.001.
74. Rodriguez Ayala F, Bartolini M, Grau R. The Stress-Responsive Alternative Sigma Factor SigB of Bacillus subtilis and its relatives: an old friend with new functions. Front Microbiol. 2020 Sep 15;11:1761. doi: 10.3389/fmicb.2020.01761
75. Heunis T, Deane S, Smit S, Dicks LMT. Proteomic profiling of the acid stress response in Lactobacillus Plantarum 423. J Proteome Res. 2014;13(9):4028–4039. doi:10.1021/pr500353x.
76. Pérez Montoro B, Benomar N, Caballero Gómez N, Ennahar S, Horvatovich P, Knapp CW, Gálvez A, Abriouel H. Proteomic analysis of lactobacillus pentosus for the identification of potential markers involved in acid resistance and their influence on other probiotic features. Food Microbiol. 2018;72:31–38. doi:10.1016/j.fm.2017.11.006.
77. Wu C, He G, Zhang J. Physiological and proteomic analysis of *Lactobacillus casei* in response to acid adaptation. J Ind Microbiol Biotechnol. 2014;41(10):1533–1540. doi:10.1007/s10295-014-1487-3.
78. Zhai Z, Douillard FP, An H, Wang G, Guo X, Luo Y, Hao Y. Proteomic characterization of the acid tolerance response in Lactobacillus Delbrueckii subsp. Bulgaricus CAUH1 and functional identification of a novel acid stress-related transcriptional regulator Ldb0677: acid tolerance response of Lactobacillus Bulgaricus CAUH1. Environ Microbiol. 2014;16(6):1524–1537. doi:10.1111/1462-2920.12280.
79. Ali SA, Singh P, Tomar SK, Mohanty AK, Behare P. Proteomics fingerprints of systemic mechanisms of adaptation to bile in Lactobacillus Fermentum. J Proteomics. 2020;213:103600. doi:10.1016/j.jprot.2019.103600.
80. Burns P, Sánchez B, Vinderola G, Ruas-Madiedo P, Ruiz L, Margolles A, Reinheimer J, de Los Reyes-Gavilán CG. Inside the adaptation process of Lactobacillus Delbrueckii subsp. lactis to bile. Lactis Bile Int J Food Microbiol. 2010;142(1–2):132–141. doi:10.1016/j.ijfoodmicro.2010.06.013.
81. Kaur G, Ali SA, Kumar S, Mohanty AK, Behare P. Label-free quantitative proteomic analysis of lactobacillus fermentum NCDC 400 during bile salt exposure. J Proteomics. 2017;167:36–45. doi:10.1016/j.jprot.2017.08.008.
82. Lee JY, Pajarillo EAB, Kim MJ, Chae JP, Kang D-K. Proteomic and transcriptional analysis of lactobacillus johnsonii PF01 during bile salt exposure by ITRAQ shotgun proteomics and quantitative RT-PCR. J Proteome Res. 2013;12(1):432–443. doi:10.1021/pr300794y.
83. Lee K, Lee H-G, Choi Y-J. Proteomic analysis of the effect of bile salts on the intestinal and probiotic bacterium Lactobacillus Reuteri. J Biotechnol. 2008;137(1–-4):14–19. doi:10.1016/j.jbiotec.2008.07.1788.
84. Wang G, Zhai Z, Ren F, Li Z, Zhang B, Hao Y. Combined transcriptomic and proteomic analysis of the response to bile stress in a centenarian-originated probiotic lactobacillus Salivarius Ren. Food Res Int. 2020;137:109331. doi:10.1016/j.foodres.2020.109331.
85. Turroni S, Bendazzoli C, Dipalo SCF, Candela M, Vitali B, Gotti R, Brigidi P. Oxalate-degrading activity in Bifidobacterium animalis subsp. Lactis: impact of acidic conditions on the transcriptional levels of the oxalyl coenzyme a (CoA) decarboxylase and formyl-CoA transferase genes. Appl Environ Microbiol. 2010;76(16):5609–5620. doi:10.1128/AEM.00844-10.

86. Kullin B, Tannock GW, Loach DM, Kimura K, Abratt VR, Reid SJ. A functional analysis of the formyl-coenzyme a (frc) gene from Lactobacillus Reuteri 100-23C. J Appl Microbiol. 2014;116 (6):1657–1667. doi:10.1111/jam.12500.
87. Koskenniemi K, Laakso K, Koponen J, Kankainen M, Greco D, Auvinen P, Savijoki K, Nyman TA, Surakka A, Salusjärvi T, et al. Proteomics and transcriptomics characterization of bile stress response in probiotic Lactobacillus Rhamnosus GG. Mol Cell Proteomics. 2011;10(2):S1–S18. doi:10.1074/mcp.M110.002741.
88. Lv L-X, Yan R, Shi H-Y, Shi D, Fang D-Q, Jiang H-Y, Wu W-R, Guo F-F, Jiang X-W, Gu S-L, et al. Integrated transcriptomic and proteomic analysis of the bile stress response in probiotic Lactobacillus Salivarius LI01. J Proteomics. 2017;150:216–229. doi:10.1016/j.jprot.2016.08.021.
89. Garcia PS, Gribaldo S, Py B, Barras F. The SUF system: an ABC ATPase-dependent protein complex with a role in Fe–S cluster biogenesis. Res Microbiol. 2019;170 (8):426–434. doi:10.1016/j.resmic.2019.08.001.
90. Ellepola K, Huang X, Riley RP, Bitoun JP, Wen ZT. Streptococcus Mutans lacking SufCDSUB is viable, but displays major defects in growth, stress tolerance responses and biofilm formation. Front Microbiol. 2021;12:671533. doi:10.3389/fmicb.2021.671533.
91. Wu T, Wang G, Tang H, Xiong Z, Song X, Xia Y, Lai PF, Ai L. Genes encoding bile salt hydrolase differentially affect adhesion of Lactiplantibacillus Plantarum AR113. J Sci Food Agric. 2022;102(4):1522–1530. doi:10.1002/jsfa.11487.
92. Yang Y, Liu Y, Zhou S, Huang L, Chen Y, Huan H. Bile salt hydrolase can improve Lactobacillus Plantarum survival in gastrointestinal tract by enhancing their adhesion ability. FEMS Microbiol Lett. 2019;366(8): fnz100. doi:10.1093/femsle/fnz100.
93. Gaucher F, Bonnassie S, Rabah H, Marchand P, Blanc P, Jeantet R, Jan G. Review: adaptation of beneficial Propionibacteria, Lactobacilli, and Bifidobacteria improves tolerance toward technological and digestive stresses. Front Microbiol. 2019;10:841. doi:10.3389/fmicb.2019.00841.
94. Hamon E, Horvatovich P, Bisch M, Bringel F, Marchioni E, Aoudé-Werner D, Ennahar S. Investigation of biomarkers of bile tolerance in *Lactobacillus casei* using comparative proteomics. J Proteome Res. 2012;11(1):109–118. doi:10.1021/pr200828t.
95. Hamon E, Horvatovich P, Izquierdo E, Bringel F, Marchioni E, Aoudé-Werner D, Ennahar S. Comparative proteomic analysis of Lactobacillus plantarum for the identification of key proteins in bile tolerance. BMC Microbiol. 2011;11(1):63. doi:10.1186/1471-2180-11-63.
96. Broadbent JR, Larsen RL, Deibel V, Steele JL. Physiological and transcriptional response of *Lactobacillus casei* ATCC 334 to acid stress. J Bacteriol. 2010;192(9):2445–2458. doi:10.1128/JB.01618-09.
97. Huang R, Pan M, Wan C, Shah NP, Tao X, Wei H. Physiological and transcriptional responses and cross protection of Lactobacillus plantarum ZDY2013 under acid stress. J Dairy Sci. 2016;99(2):1002–1010. doi:10.3168/jds.2015-9993.
98. Ma X, Wang G, Zhai Z, Zhou P, Hao Y. Global transcriptomic analysis and function identification of malolactic enzyme pathway of Lactobacillus paracasei L9 in response to bile stress. Front Microbiol. 2018;9:1978. doi:10.3389/fmicb.2018.01978.
99. O'Connor A, McClean S. The role of universal stress proteins in bacterial infections. Curr Med Chem. 2017;24 (36):3970–3979. doi:10.2174/0929867324666170124145543.
100. Samanta S, Biswas P, Banerjee A, Bose A, Siddiqui N, Nambi S, Saini DK, Visweswariah SS. A universal stress protein in mycobacterium Smegmatis sequesters the CAMP-Regulated lysine Acyltransferase and is essential for biofilm formation. J Biol Chem. 2020;295 (6):1500–1516. doi:10.1074/jbc.RA119.011373.
101. Adhikari AA, Ramachandran D, Chaudhari SN, Powell CE, Li W, McCurry MD, Banks AS, Devlin AS. A gut-restricted lithocholic acid analog as an inhibitor of gut bacterial bile salt hydrolases. ACS Chem Biol. 2021 Aug 20;16(8):1401–1412. doi: 10.1021/acschembio.1c00192
102. Adhikari AA, Seegar TCM, Ficarro SB, McCurry MD, Ramachandran D, Yao L, Chaudhari SN, Ndousse-Fetter S, Banks AS, Marto JA, et al. Development of a covalent inhibitor of gut bacterial bile salt hydrolases. Nat Chem Biol. 2020;16(3):318–326. doi:10.1038/s41589-020-0467-3.